

Stability of the West Slope of Government Hill Port Area of Anchorage, Alaska

By DAVID J. VARNES

CONTRIBUTIONS TO ENGINEERING GEOLOGY

GEOLOGICAL SURVEY BULLETIN 1258-D

*An evaluation of the stability of
gravel-capped bluffs of Bootlegger
Cove Clay under static and
seismic conditions*



UNITED STATES DEPARTMENT OF THE INTERIOR

WALTER J. HICKEL, *Secretary*

GEOLOGICAL SURVEY

William T. Pecora, *Director*

CONTENTS

	Page
Abstract.....	D1
Introduction.....	1
Topography, geology, and development of the port area.....	2
Flow slide and closed depression.....	16
Response of the port area to the March 27, 1964, earthquake.....	16
Stability analyses.....	19
General procedure.....	19
Methods used.....	22
Boring line 1.....	30
Old slides.....	30
Circular arc failure, static.....	33
Failure along a flat surface.....	35
Boring line 2.....	40
Old slides.....	40
Circular arc failure.....	42
Failure along a flat surface.....	42
Summary of stability.....	44
Boring line 1.....	44
Boring line 2.....	47
General remarks.....	47
Other engineering geologic problems.....	48
Suggestions concerning future development.....	49
Suggestions for future studies.....	50
References.....	51
Appendix A.....	55
Appendix B.....	57
Appendix C.....	59

ILLUSTRATIONS

	Page
PLATE	1. Topographic map of port area of Anchorage, Alaska, 1966, on which is superposed the Alaskan Engineering Commission's map of Ship Creek, 1914.....In pocket 2. Section along lines A-A' and B-B', Government Hill, Anchorage, Alaska.....In pocket 3. Cross sections along boring lines 1 and 2 and logs of borings.....In pocket
FIGURE	1. Index map of the port area in the northern part of the city of Anchorage, Alaska, as of 1962.....D3 2. Aerial photograph of the port area as seen from over the main part of the city of Anchorage.....4

	Page
FIGURE 3. Aerial photograph of the port area of Anchorage as seen from over Knik Arm.....	D5
4-9. Photographs:	
4. Coal-bunker site as seen from marine ways, July 1, 1917.....	7
5. Ships ways, March 1, 1917.....	7
6. View northward from Government Hill, early 1918.....	8
7. Coal-dock site, June 27, 1918.....	9
8. Anchorage harbor as seen from Government Hill, November 7, 1921.....	10
9. Terminal yards as seen from end of temporary trestle, August 20, 1918.....	10
10-14. Photographs showing vertical aerial views of the port area, Anchorage:	
10. August 7, 1942.....	11
11. August 8, 1950.....	12
12. May 17, 1962.....	13
13. June 1, 1964.....	14
14. May 2, 1967.....	15
15. Sketch showing ground cracks caused by the March 27, 1964, earthquake and scarps of old landslides.....	18
16. Photograph of view northeastward over the south end of the port area as seen from above Ship Creek after the earthquake of March 27, 1964.....	19
17-29. Graphs:	
17. Stability analysis of uniform slope by force polygons.....	23
18. Force polygon for slice 1.....	24
19. Force polygon for slice 4.....	25
20. Theoretical particle motion for a Rayleigh wave.....	27
21. Stability analysis of pre-1916 slide.....	31
22. Determination of position of former crest of slope, boring line 1.....	32
23. Force-polygon stability analysis, arc <i>ABCJ</i> , line 1, static conditions.....	36
24. Force-polygon stability analysis, arc <i>ABCN</i> , line 1, static conditions.....	37
25. Force-polygon stability analysis, arc <i>ABCJ</i> , line 1, seismic coefficients of 0.15 horizontal and 0.15 vertical.....	38
26. Determination of depth of potential failure surface <i>LM</i> , boring line 1.....	39
27. Stability analysis by moments about center of arc <i>RSP</i> , boring line 2, static conditions.....	44
28. Graphical determination of active pressure E_a on <i>GD</i> , boring line 2.....	45
29. Graphical determination of active pressure E_a on <i>NC'</i> , boring line 2.....	46

TABLES

TABLE		Page
	1. Basic data for analysis of potential failure along arc <i>ABCJ</i> , boring line 1-----	D34
	2. Numbered items in logs of borings ARR-2A, ARR-2B, and ARR-2C used to correlate between borings-----	41
	3. Stability analysis by moments about center of arc <i>RSP</i> , boring line 2, static conditions—moments of slices-----	43
	4. Calculation of stability along arc <i>RSP</i> , boring line 2-----	43

CONTRIBUTIONS TO ENGINEERING GEOLOGY

STABILITY OF THE WEST SLOPE OF GOVERNMENT HILL PORT AREA OF ANCHORAGE, ALASKA

By DAVID J. VARNES

ABSTRACT

Government Hill rises about 100 feet above an industrial and port area built on a filled-in tidal flat. The nearly horizontal top of the hill is occupied by a residential district. A capping of 35-45 feet of sand and gravel is underlain by Bootlegger Cove Clay, which consists of clayey silt containing thin beds of fine to medium sand. Almost continuous old landslides form the west- and northwest-facing slopes. Some petroleum storage tanks and residences are on, or adjacent to, old landslides.

Slope-stability safety factors were computed in the vicinity of two lines, along which borings were made and samples tested. Under static conditions the slope at line 1 seems to be stable so long as the toe is not removed to make level ground; the lower part of the slope at line 2 seems to be on the verge of failure along an assumed circular arc. Under seismic conditions both slopes appear susceptible to failure along flat zones in the Bootlegger Cove Clay, if seismic coefficients are assumed to be 0.05 for line 1 and 0.035 for line 2 in stability computations. No major slope failure in the vicinity of lines 1 and 2 accompanied the 1964 earthquake.

Topographic and geologic environments indicate that further industrial development should proceed with caution.

INTRODUCTION

The present study was made in response to a request from The Alaska Railroad to the U.S. Geological Survey for an evaluation of the propriety of continued industrial expansion on land within The Alaska Railroad Terminal Reserve and nearby.

The purpose of this report is to make available to the public the information obtained and the conclusions drawn therefrom and to discuss factors that influence the method and reliability of obtaining conclusions from the available data.

The report is based on field examinations made June 8-12, 1966, in company with E. B. Eckel and Ernest Dobrovolsky, on fieldwork of September 19-October 3, 1966, and of May 1-June 4, 1967, on discussions with the staff of The Alaska Railroad, and on review of both published and unpublished material pertinent to the area and its problems.

The advice and criticism of my colleagues W. R. Hansen, H. W. Olsen, and D. S. McCulloch and of Ruth A. M. Schmidt of Anchorage have been very helpful. Prof. H. Bolton Seed of the University of California greatly aided the investigation with his advice and by review of an earlier report placed in open file (Varnes, 1968). Much useful information in the form of maps, photographs, and unpublished reports was made available from the files of The Alaska Railroad.

In the fall of 1966 a detailed topographic map of the port area was prepared for The Alaska Railroad by Jay Whiteford & Associates. During late 1966 and early 1967 a drilling, sampling, and soils-testing program in an area of immediate interest (along boring lines 1 and 2, pl. 1) was made by ACLW (Adams, Corthell, Lee, Wince & Associates), a consultant engineering firm, under contract to The Alaska Railroad. Almost all the basic data used in this report for stability analyses, such as the geometry of the ground surface and the physical properties of the materials, were derived from the Whiteford map and the ACLW investigations.

TOPOGRAPHY, GEOLOGY, AND DEVELOPMENT OF THE PORT AREA

The port area as of 1962 is shown in figure 1 and as of August 11, 1963, in figures 2 and 3. Many of the natural features and structures referred to in text are identified in figure 14. The port area consists of a strip of flat ground that extends from sea level to about 20 feet above high tide. It is $1\frac{1}{2}$ miles long and as much as half a mile wide; it fronts on Knik Arm northward from Ship Creek and is bordered on the northeast and southeast by wooded bluffs about 100 feet high. Plate 1 shows a part of the boundary of The Alaska Railroad Terminal Reserve, which includes the southern part of the port area.

The flats in front of the bluff are underlain by estuarine silt, peat, muskeg, and artificial fill. The bluffs are formed of Bootlegger Cove Clay, an estuarine-marine deposit 50 feet thick or more that consists largely of Pleistocene silty clay interbedded with thin lenses of sand and overlain by about 40 feet of glacial outwash sand and gravel.

Bluffs such as these, exposed to erosive action of strong tidal currents in a region of active freezing and thawing, are almost sure to be progressively modified by slumping. Landsliding has long been the active agent of cliff retreat wherever fine-grained glacial deposits border Knik Arm, and the resulting landforms and deposits are easily seen and interpreted where not obscured by brush and trees or by manmade modifications. Owing to progressive filling in the port area since 1918, the tide can no longer reach the foot of the slopes and

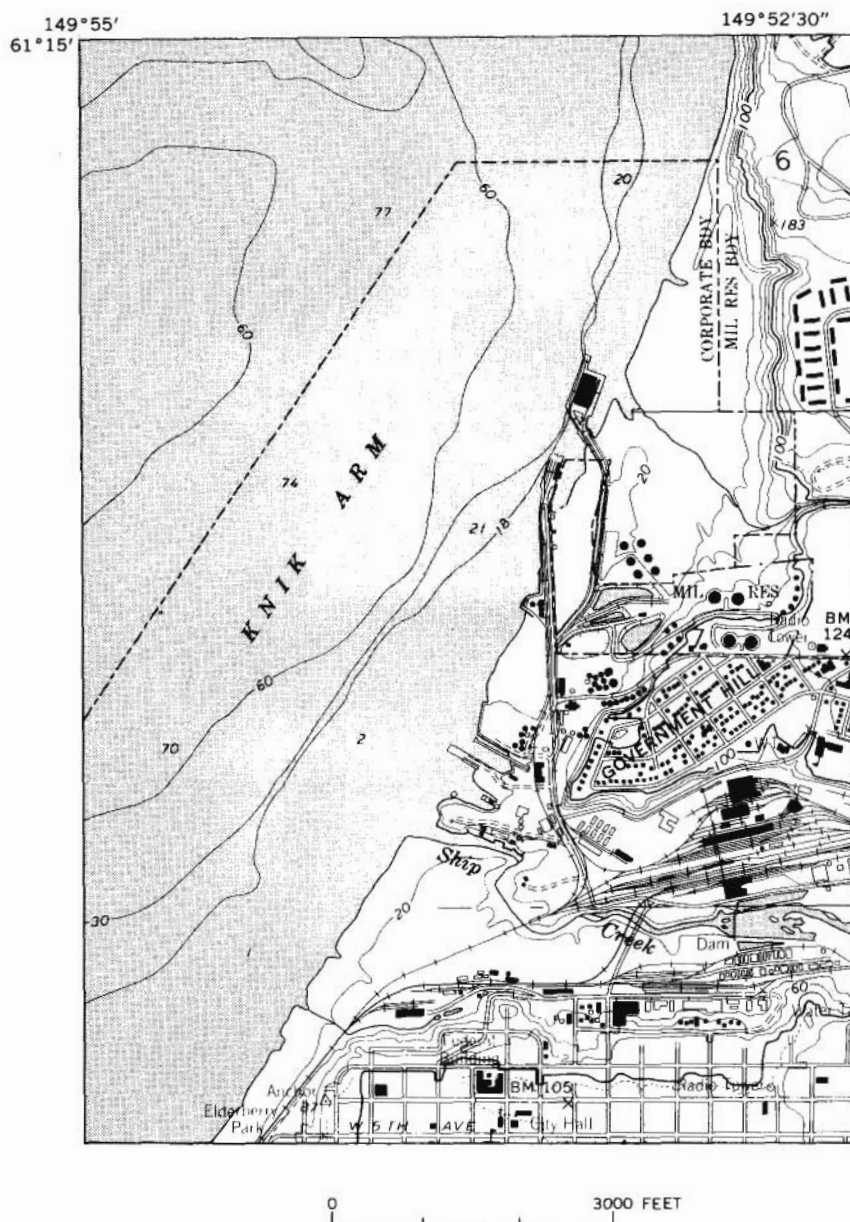


FIGURE 1.—Location of the port area in the northern part of the city of Anchorage, Alaska, as of 1962.



FIGURE 2.—View northward toward the port area as seen from over the main part of the city of Anchorage, Alaska. Business district is in right foreground. Ship Creek flows (to the left) into Knik Arm of Cook Inlet. Government Hill rises beyond Ship Creek in right center. In the middle distance is the Army Dock, and beyond is the then newly constructed City Dock. Photographed August 11, 1963, by Steve McCutcheon, Anchorage.

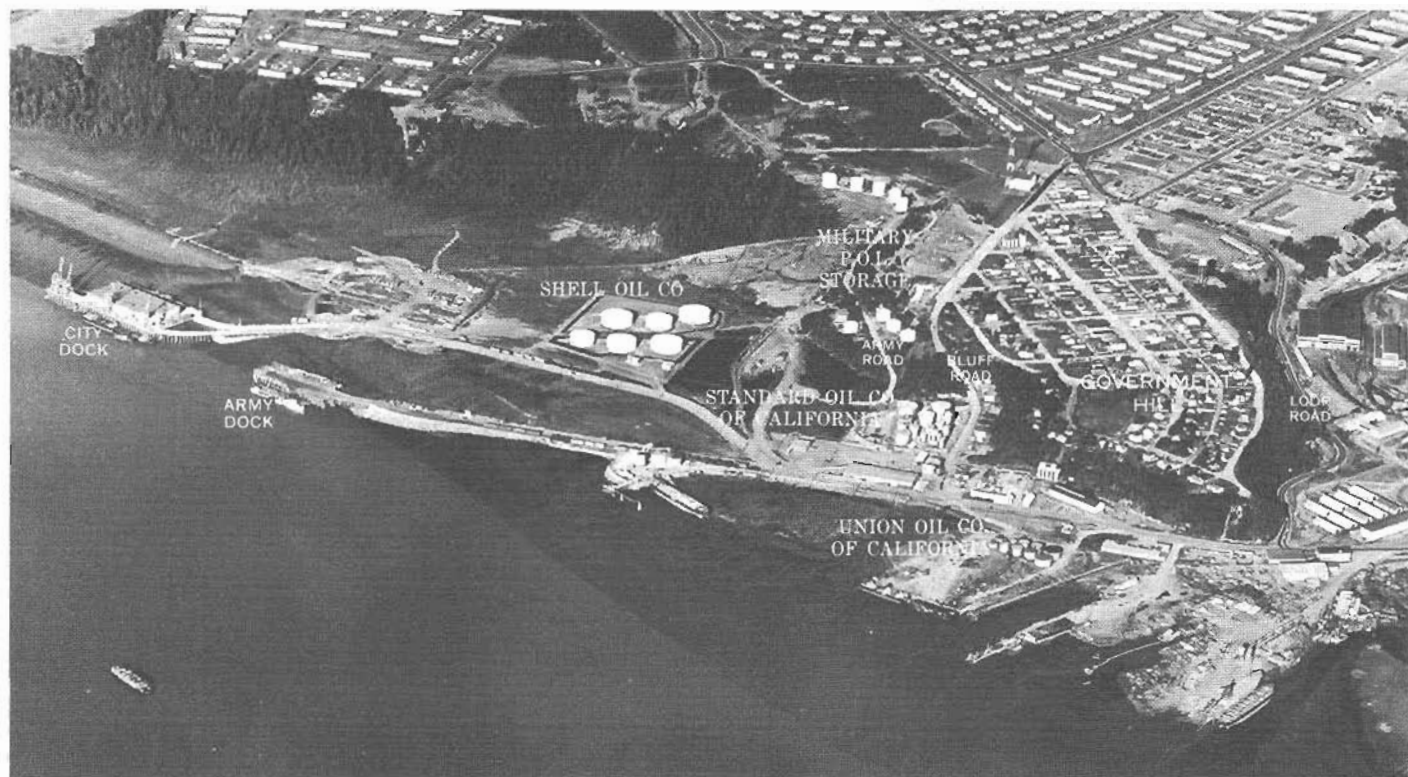


FIGURE 3.—View eastward toward the port area of Anchorage, Alaska, as seen from over Knik Arm. Photographed August 11, 1963, by Steve McCutcheon, Anchorage.

remove slide material. The cessation of erosion has tended to help stabilize the slopes.

The surficial geology of the Anchorage area has been described by Miller and Dobrovolsky (1959), and the relation of the geology to effects of the March 27, 1964, earthquake by Hansen (1965) and by others. The physical properties and seismic response of the Bootlegger Cove Clay and other surficial deposits have been the subject of many studies since the earthquake and the extensive landsliding in 1964. Particularly pertinent to this area are the investigations by Shannon and Wilson, Inc. (1964).

All the slopes forming the north side of the valley of Ship Creek and the west side of Government Hill—from Loop Road around to the military petroleum-products storage tanks and beyond—appear to have slid at some time in the past. Many of the old scarps are still visible, but construction and regrading for roads, houses, and industrial development have obscured much of the original form of the slopes and of the flats in front of them. It seemed useful, therefore, to trace the changes that have occurred, after attempting to determine how The Alaska Railroad Terminal Reserve and other parts of the port area looked before development.

Plate 1 shows part of a topographic map prepared in 1914 by the Alaskan Engineering Commission (1916, map 13) superposed on the 1966 topographic map. The irregular hummocky topography produced by old slides is well shown on the earlier map, particularly the old flow-type slide at the present site of the Standard Oil of California Terminal Yard and the smaller slide in the area crossed by boring line 1.

Figures 4–9 are photographs taken by the Alaskan Engineering Commission of parts of the present Alaska Railroad Terminal Reserve in 1917–21, after the initial settlement in 1915. The approximate positions from which these photographs were taken are indicated on plate 1. The toe of the flow slide can be seen (on the right) in figures 4, 6, and 7. The size of the trees growing on the slide indicates that the flow was probably several decades old in 1918, yet trees either leaning or fallen at the toe indicate some continued movement and tidal erosion. The slide in the area of boring line 1 is shown (on the left) in figure 5 and in (foreground) figures 6 and 8. It, too, looks old, judging from the upright mature conifers shown in figure 6, although movement during growth of the trees cannot be ruled out. For reference, three trees are identified by letters in figures 6 and 8. Figures 5 and 9 show that almost all the trees were removed from the nose of Government Hill at an early date. Figure 9 shows the discharge pipe of the dredge operating at the site of Army Dock (then called Ocean Dock); the pipe emptied landward from the railroad trestle and

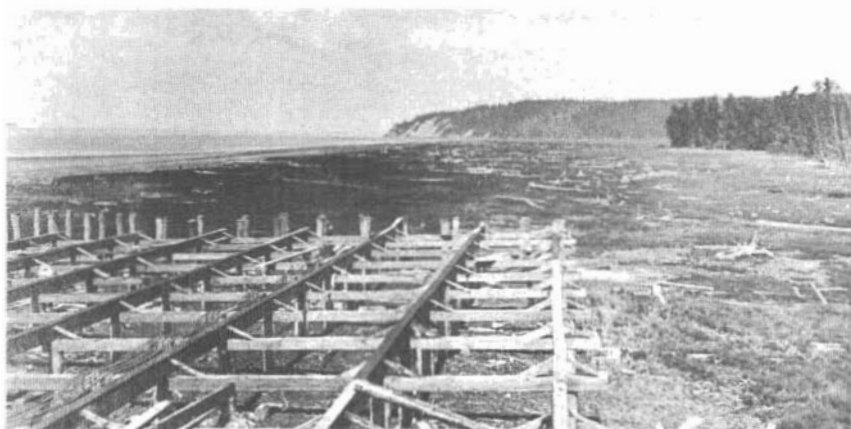


FIGURE 4.—Coal-bunker site as seen from marine ways, Anchorage, Alaska, July 1, 1917. Toe of flow slide is in the woods (on the right). Photograph by Alaskan Engineering Commission.



FIGURE 5.—Ships ways, Anchorage, Alaska. Nose at southwest end of Government Hill is visible (on the left) with landslide deposits at the toe of the slope. Photograph by Alaskan Engineering Commission, March 1, 1917.

illustrates the beginning of the process of artificial filling that has continued along the shore ever since.

Figures 10-14 are vertical aerial views of the mouth of Ship Creek and the port, showing approximately the same area to the same scale at succeeding intervals, beginning with the earliest available photographs taken in August 1942 and ending with photographs taken in May 1967. Some landmarks and areas of interest are identified in figure 14.

The elongated triangular flat of the port area shown in figure 10, is modified only by the white trace of the Elmendorf Air Force Base sewer outfall and by the developed areas near the southwest corner of Government Hill. The west slope of Government Hill is clearly broken into long furrows by slide blocks and is interrupted by the nearly circular outline of the flow slide. North of the outfall the crest of the slope consists of a half dozen or more shallow arcs marking the heads of old slides. Faint remnants of the removed material show on the flat as brush-covered lobes of somewhat higher ground supporting a growth of bushes.



FIGURE 6.—View northward from Government Hill, probably in early 1918. Future site of Independent Lumber Co. warehouse is about at the foot of the landslide deposits beyond tree marked A. Toe of flow slide is in middle distance at right. Letters identify the same trees shown in figure 8. Photograph by Alaskan Engineering Commission.



FIGURE 7.—Coal-dock site, Anchorage, Alaska, June 27, 1918. Note fallen trees at toe of flow slide in the middle distance at right. Railway cars are on the coal-storage bunker. Photograph by Alaskan Engineering Commission.

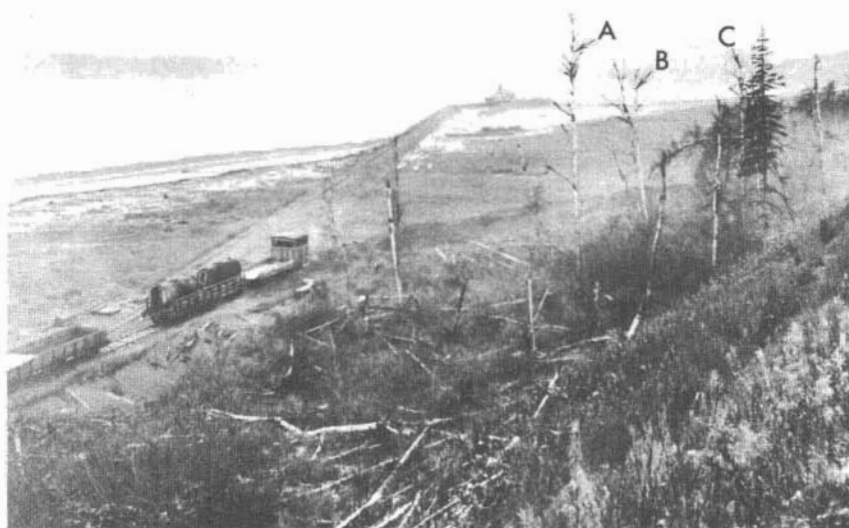


FIGURE 8.—Anchorage harbor as seen from Government Hill, November 7, 1921. Note that the coal-storage bunker has largely been removed. Letters identify the same trees shown in figure 6. Photograph by Alaskan Engineering Commission.



FIGURE 9.—Terminal yards as seen from end of temporary trestle at high tide, August 20, 1918. Photograph by Alaskan Engineering Commission.

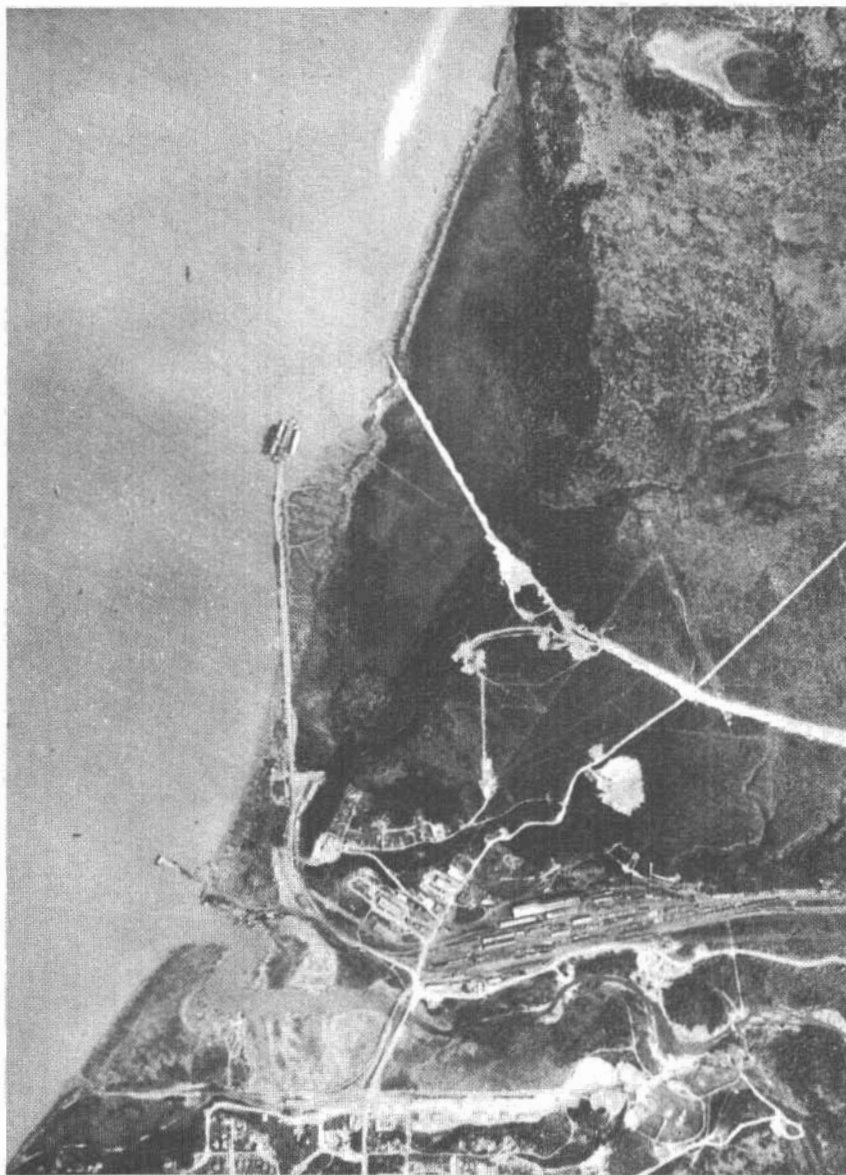


FIGURE 10.—Vertical aerial view of the port area, Anchorage, Alaska, from trimetrogon photograph by U.S. Army Air Force, mission 2-2011, flight 34, frame 4V, August 7, 1942.



FIGURE 11.—Vertical aerial view of the port area, Anchorage, Alaska, from photograph by U.S. Geological Survey, 102VV, M373, August 8, 1950.



FIGURE 12.—Vertical aerial view of the port area, Anchorage, Alaska, from photograph by U.S. Geological Survey, 1-97, GS-VAFC, May 17, 1962.

As embankments were built onto the flat, particularly north of the Standard Oil of California development on the flow slide, drainage to the sea was increasingly impeded, and ponds formed between the embankments or between the embankments and the slope (figs. 11, 12, 13). Also, greatly increased runoff from the expanded development at Elmendorf Air Force Base during 1950-62 cut a sharp-walled ravine (shown in the right-central part of fig. 12) and no doubt contributed to the formation of ponds in the flat area.

Hydraulically placed fill derived from dredging for the new City Dock, built in 1961, occupies much of the light-colored area southeast of City Dock shown in figure 12. This fill also apparently helped create an impervious barrier to waters that formerly flowed from the slopes to the sea. A drainage ditch was constructed in 1962 or 1963 to divert runoff to the north around the growing fills east of City Dock. Nevertheless, in the summer of 1966 much of the area



FIGURE 13.—Vertical aerial view of the port area, Anchorage, Alaska, from photograph by Air Photo Tech, Anchorage, ROP 1-3, June 1, 1964.

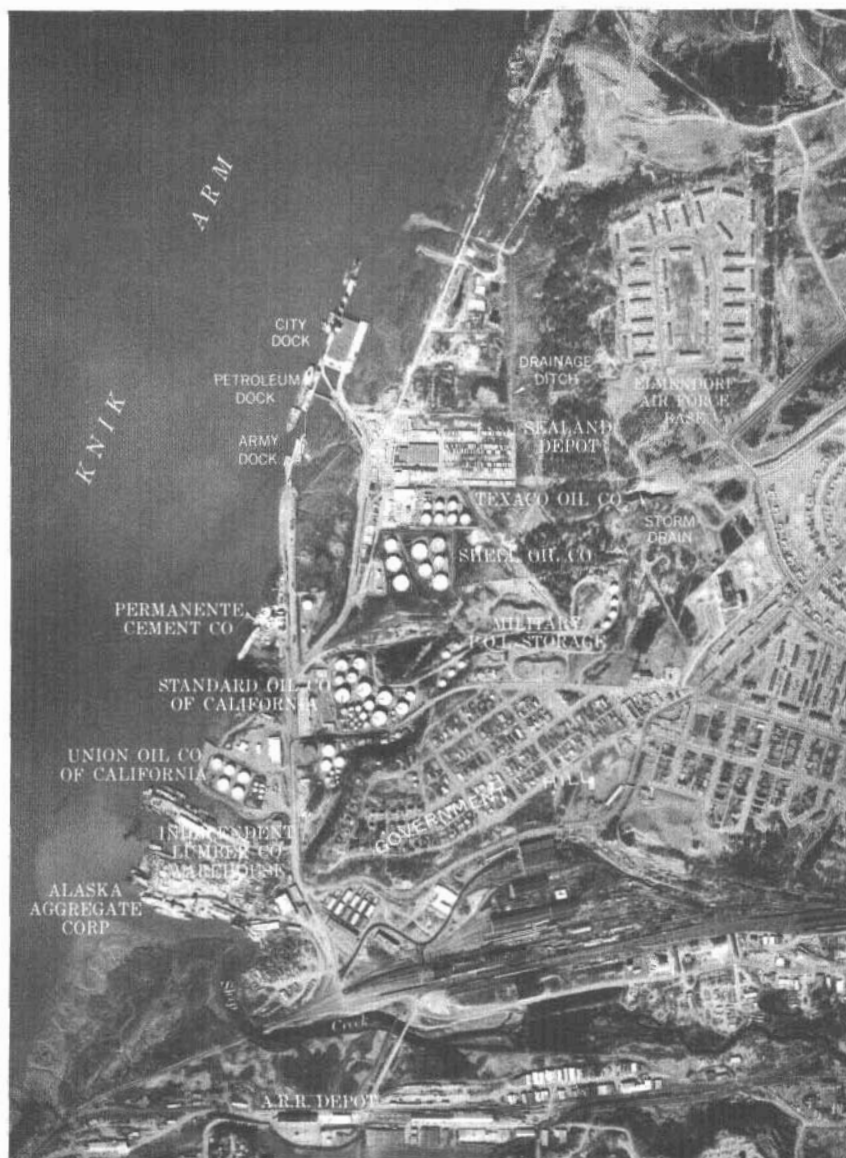


FIGURE 14.—Vertical aerial view of the port area, Anchorage, Alaska. Note large new tanks in the Union Oil Co. of California area, both near the bluff of Government Hill and on fill next to Knik Arm; a new group of large tanks in the Standard Oil of California area, some in a site formerly occupied by a pond; repairs and additions to the Shell Oil Co. tanks; and a new group of seven large and four small tanks erected by Texaco Oil Co. From photograph by Air Photo Tech, Anchorage, ANC 1-2, May 2, 1967.

p. 44-47), Brevdy (1964, p. 15), National Board of Fire Underwriters and Pacific Fire Rating Bureau (1964, p. 29-30), Stephenson (1964, p. 11-12, figs. 31-34, 37-39), Steinbrugge, Manning, and Degenkolb (1967, p. 122-124), and Eckel (1967, p. B8-B9).

Within the area of the port included in The Alaska Railroad Terminal Reserve west of Government Hill, damage by the earthquake was reported as follows: Army Dock was rendered unusable; a cement storage bin was overturned at the Permanente Cement Co.; the top of a storage tank collapsed at the Shell Oil Co. tank farm; three storage tanks in the Standard Oil Co. tank farm bulged around the base and leaked, one horizontal tank was thrown off its supports, and empty tanks rocked and tore catwalks; ground cracked in vicinity of Union Oil Co. asphalt plant and farther south in the filled land to Ship Creek; a crane was thrown down a cement storage bin was toppled at the Alaska Aggregate Corp. dock facilities. The whole port area subsided, probably not uniformly, 1-2½ feet.

Studies made by the writer in the field in 1966 and 1967 and of aerial photographs taken shortly after the earthquake added a few details to the pattern of ground cracking presented by Hansen (1965); his map with additions is shown in figure 15.

A crack in the fill in the area of the Union Oil Co. asphalt tanks is designated as No. 1 in figure 15. Plate 1 shows a line of hachures that passes under these same tanks. This line, transferred from the 1914 topographic map, indicates the break in slope between grass-covered marsh, to landward, and the bare inclined slippery clay surface, to seaward, that extends to the surface of the water. This boundary is shown (left-center) in figures 4 and 8. The underlying shore topography seems likely to have influenced cracking in the fill during the 1964 earthquake, for most of the cracks west of Ocean Dock Road (fig. 15) are at or below the break in slope of the old shore.

A crack east of the Independent Lumber Co. warehouse at the base of the slope (fig. 15, No. 2; fig. 16, upper right) crossed boring line 1. The crack provided some direct evidence for the potential instability under seismic shaking that is inferred in the analyses to follow. Regrading since the earthquake has obscured the crack.

Plate 2 shows section *B-B'* along boring line 1 extended westward, with a slight change in direction at boring ARR-1D, across Ocean Dock Road and through the Union Oil Co. tank farm. The large tanks were erected after the 1964 earthquake. The depth to which the sheet pile bulkhead extends at the west edge of the fill is not known by the writer.

between the slopes and the tank farms and fills in the port area was covered by a nearly continuous body of standing water.

Rapid development of the port area during the period June 1964–May 1967 (fig. 14) resulted largely from the increased use of the port following the 1964 earthquake. New petroleum dock, handling, and storage facilities were constructed in part to replace those destroyed by the earthquake at other coastal cities.

FLOW SLIDE AND CLOSED DEPRESSION

The Standard Oil of California tank farm is built in large part on the disk-shaped flow slide discussed previously. This area should be carefully watched for signs of movement. One of the areas apparently most active within The Alaska Railroad Terminal Reserve is south of Bluff Road at the foot of the slope back of the line of asphalt tanks. There, a wooden retaining wall was displaced and, in September 1966, was observed to be crowding adjacent steam lines.

The flow slide appears to be related to the closed depression directly to the south on Government Hill. Although the depression could be a kettle that resulted from the melting of ice within the glacial outwash gravels, it might instead be a much-modified remnant of a grabenlike depression associated with the landslide. The ground between the depression and the crest of the hill to the north above the slide is inclined toward the depression in a way suggesting that the depression is over an old slide block. To test this hypothesis an auger hole was drilled in May 1967 by the U.S. Geological Survey, under the direction of W. W. Barnwell, close to the crest of the hill. The top of the clay was found to be significantly higher here than in Shannon-Wilson boring F-110A closer to center of the depression. The writer favors the hypothesis that the depression is a graben, rather than a kettle, and interprets the available information as shown in section A-A', plate 2.

The strong possibility that the depression is an old graben requires that the potential effects of grading around or filling in the depression be closely evaluated so as to avoid reactivating movement.

RESPONSE OF THE PORT AREA TO THE MARCH 27, 1964, EARTHQUAKE

The effects of the March 27, 1964, earthquake in the port area have been reported by Engineering Geology Evaluation Group (1964, p. 22, fig. 12), Hansen (1965, p. A27–A29, fig. 14), Fisher and Merkle (1965, p. 81–82, figs. 227–238, 243), Berg and Stratta (1964,

failure surface are tried. The failure surface with the lowest safety factor is probably the most dangerous one. The search for the slip surface with the lowest safety factor can take an unwarranted amount of time, if the slope has already been determined to be marginally stable, unless specific construction designs are under consideration.

METHODS USED

Two methods were used to derive estimates of the stability of the slopes near boring lines 1 and 2. These methods differ in the assumed geometry of the potential surface of failure, in the way that the forces acting on the potential slide mass are resolved into those driving and those resisting, and in the division of the slide mass into circular sectors, vertical slices, wedges, or other geometrical parts for convenience of analysis.

The first method, that of determining the driving and resisting forces acting on an assumed cylindrical slip surface, is so well known as to require little discussion. It is here employed in two following variations:

1. Calculation, in a vertical longitudinal 1-foot-thick section through the slide, of the forces acting on the base of vertical slices.
2. Calculation of moments about the center of rotation, in a similar section, of the driving forces acting at the center of gravity and of resisting forces acting at the base of the slide along the potential slip surface.

The second variation is restricted to cylindrical slip surfaces that appear as circular arcs (or, in special instances, logarithmic spirals) in the plane of the section, whereas the first variation can be used with irregularly curved slip surfaces. The two variations are mathematically equivalent. In each, the resisting forces are assumed to act along the base of the slide, and both variations may be included under the general term "method of base forces."

The second method, termed the "method of force polygons," has long been in use. It was employed by Fellenius and others in early expositions of the Swedish way of summing up forces on a slide mass bounded by a circular arc. Owing to its versatility, the method has been improved and was described more recently by Seed (1966), Lowe (1967), and other writers.

In the force-polygon method the potential slide mass is also divided into segments that lie above some assumed surface of failure, as shown graphically in figure 17. The forces acting on each segment are similar to those shown acting on slice 1. Included are the forces exerted by each slice on its neighbor across the vertical boundaries between them. These E forces, which are neglected (or assumed to

total zero) in the method of base forces, are assumed, following Lowe (1967), to act in a direction that is the average between the inclination of the ground surface and the inclination of the slip surface at the slice boundary. In the example shown the force E_{1-2} acting between slices 1 and 2 acts at an angle to the horizontal of

$$\frac{1}{2}[(33\frac{3}{4}+0)/2+39\frac{3}{4}]=28.3^\circ.$$

The resisting strength, S_D , of the material developed along the slip surface is

$$S_D = C/F + (N \tan \phi)/F,$$

where C and ϕ are, respectively, the experimentally determined values for cohesion and angle of internal shearing resistance of the material;

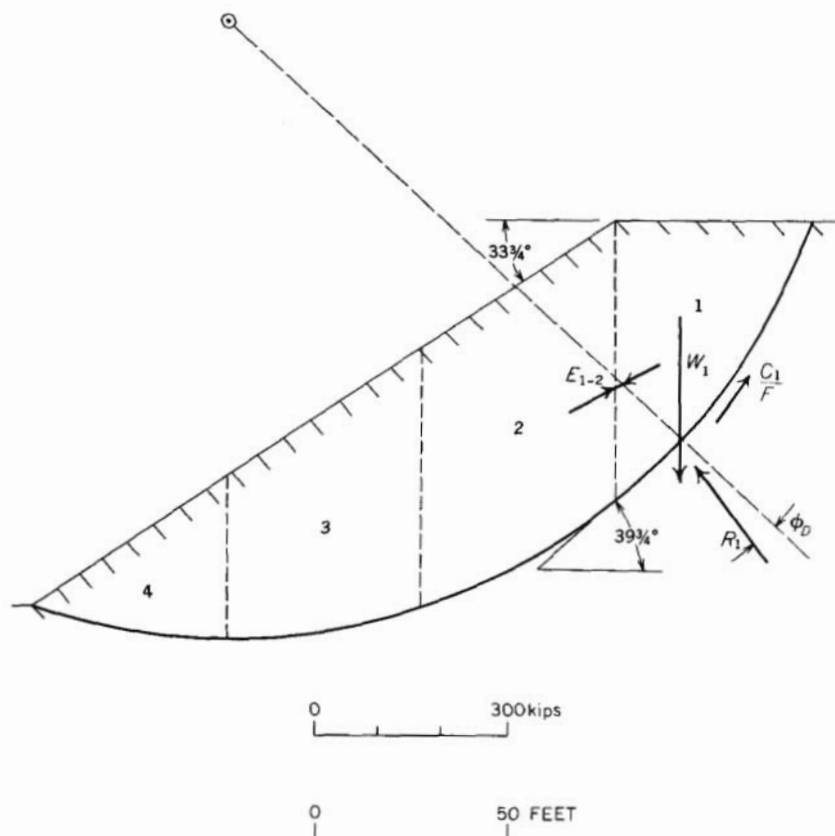


FIGURE 17.—Uniform slope of homogeneous material divided into slices for analysis of stability, by force-polygon method and with the assumption that potential failure is along a circular arc. $\gamma=125$ pcf (pounds per cubic foot); $c=1,000$ psf (pounds per square foot); $\phi=10^\circ$.

N is the normal force on the slip surface; and F is the factor of safety assumed for the analysis.

It is convenient to show the reaction, R , on the slip surface as acting at an angle ϕ_D to a normal to the slip surface, where ϕ_D is defined by

$$\tan \phi_D = (\tan \phi)/F.$$

Thus,

$$S_D = C/F + N \tan \phi_D,$$

and the vector resultant of N and $N \tan \phi_D$ is R .

The forces W and C/F are known in both direction and amount; the force R is known in direction (from ϕ and F) but not in amount; conversely, the E force is initially known in neither amount nor direction. The static equilibrium of slice 1 is indeterminate until the direction of E is assumed, either as previously described or according to one of several other rules proposed. Once the direction of E is fixed, a closed polygon of forces can be constructed. Figure 18 shows such a polygon for slice 1, made under the assumptions that the safety factor $F' = 0.9$ (solid lines) or $F'' = 1.1$ (dashed lines).

Successive polygons can be constructed for the slices in order; that for slice 2 incorporates force E_{1-2} directed now from 1 toward 2, and the subsequent E forces are similarly transferred from polygon to

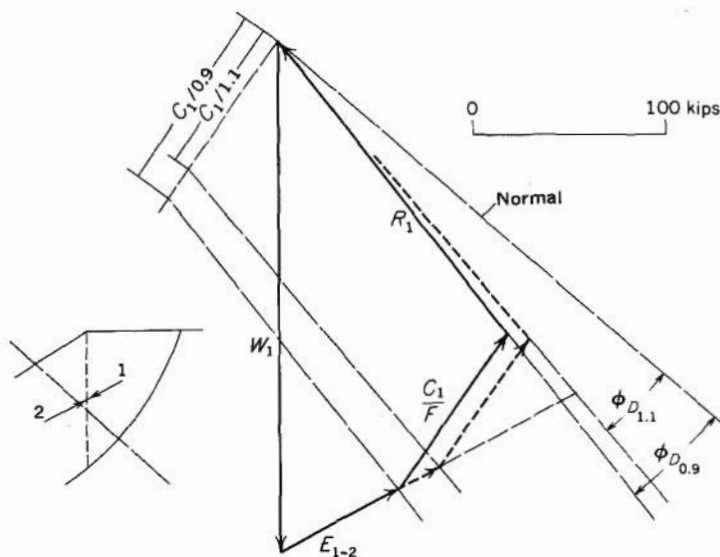


FIGURE 18.—Force polygon for slice 1 of the potential slide shown in figure 17, assuming factor of safety, $F' = 0.9$ (solid lines) or $F'' = 1.1$ (dashed lines).

polygon. The final polygon—that for slice 4—is shown in figure 19. This polygon does not close; the assumption that $F'=0.9$ has led to an excess of resistance represented by length D_1 ; and the assumption that $F''=1.1$ to a deficiency given by distance D_2 . A close estimate of the true value of the safety factor, F_t , can be obtained from the expression:

$$F_t = F' + (F'' - F') D_1 / (D_1 + D_2), \text{ or}$$

$$F_t = 1.03.$$

This "bracketing" procedure appears to be quicker and simpler than the procedure outlined by Seed (1966) and by Lowe (1967) of repeated trials with various safety factors until closure is attained.

The graphically constructed polygons may be laid out in a chain, at a scale appropriate to the accuracy of the input data, and on a sheet near the geologic cross section of the slide, so that directions of normals, and so on, may conveniently be transferred.

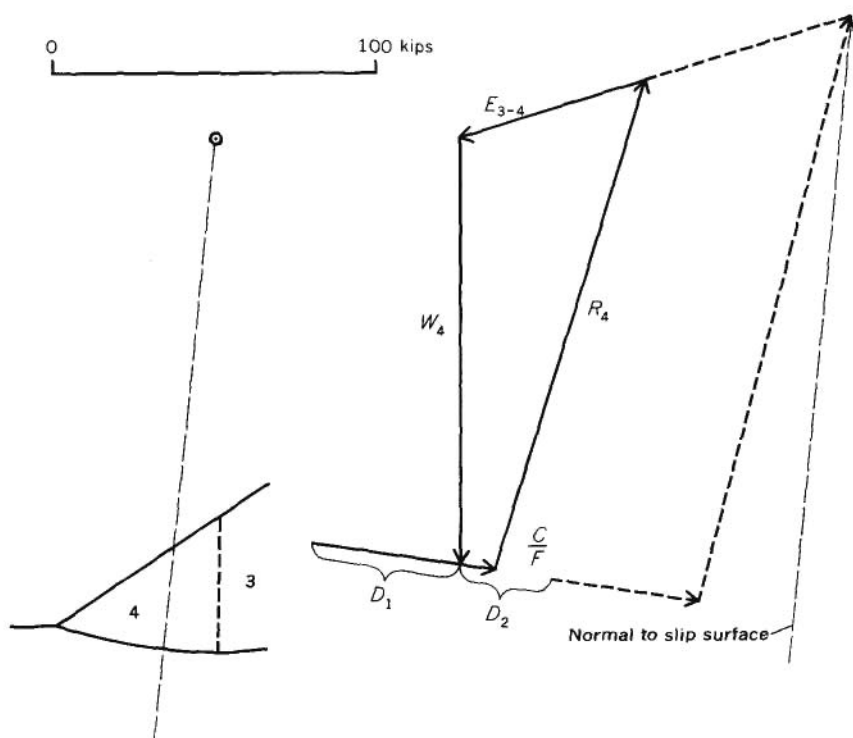


FIGURE 19.—Force polygon for slice 4 of the potential slide shown in figure 17, assuming factor of safety equals 0.9 (solid lines) or 1.1 (dashed lines). Assumption $F'=0.9$ leads to an excess of resistance represented by distance D_1 ; whereas assumption $F''=1.1$ leads to a deficiency given by distance D_2 . True factor of safety has an intermediate value of 1.03.

The polygon of forces method is easily adapted to handle irregular topography, irregular assumed slip surfaces, variation of physical properties in layered systems, pore water pressure, and static inertial forces intended to simulate the effect of seismic vibration.

Consideration of the possible effects of earthquakes on the slopes of The Alaska Railroad Terminal Reserve must weigh heavily in decisions concerning industrial development. Yet prediction of the dynamic behavior of even simple uniform slopes and embankments under completely specified vibratory stimulation has only very recently become a possibility through the most advanced methods of dynamic soil testing and analysis as presented, for example, by Seed (1966, 1967), Seed and Chan (1966), and Clough and Chopra (1966). The method used in this report is crude, indeed; yet, even it requires a little explanation, as follows.

No strong motion records of the great March 27, 1964, earthquake were obtained within Alaska. However, the physical effects of the earthquake and many eyewitness accounts suggest that much of the severest shaking was produced by large-amplitude surface waves or by interference, or resonance phenomena, associated with multiple trains of such waves. The severe disturbances appear to have had periods somewhere in the range 0.7–2 seconds and wavelengths of a few tens to a few hundreds of yards.

Three principal types of surface waves commonly result from seismic or explosive energy release. Waves of the Rayleigh and Sezawa types involve orbital particle motion in a vertical plane normal to the wave front. They produce accelerations that are directed not only forward and backward but also up and down; the direction of rotary motion at the surface is opposite in these two types. In waves of the Love type, accelerations are dominantly in a horizontal plane and oriented transversely to the direction of propagation. Owing to the more unfavorable directions of acceleration, the Rayleigh or the Sezawa waves may offer more potential danger to slopes across their paths of propagation than do the Love waves.

Little is definitely known about the propagation, reflection, and refraction of complex surface waves in layered systems of real earth materials or about the stresses these waves induce in a slope across their path. Insofar as the actual ground motion may be represented by a Rayleigh wave, for example, an examination of the motions produced by such a wave aids in understanding the problem of slope stability. The theoretical displacements and accelerations produced by the passage of a Rayleigh wave close to the surface, originating from a distant source, are shown in figure 20 (from Cagniard, 1962). The maximum ground acceleration is directed upward and backward at 45° to the horizon, and the maximum inertial force generated in a slope

opposing such acceleration would be directed downward and outward at 45° such as to virtually add its effects to the natural driving forces that seek to make the slope fail. The real conditions are undoubtedly much more complex, owing not only to irregular motions of the incoming waves but also to the geometry of the slope, and the shear moduli, damping characteristics, and other physical properties of the materials within it.

The dynamic effect of an earthquake upon the slope is here roughly approximated by assuming an additional static force to operate on each element of the potential slide. This inertial force, I , is computed from

$$I = k_s W,$$

where W is the weight of the element, and k_s is a seismic coefficient.

In the stability analyses of this report, the direction of I is generally taken to be downward and outward at 45° , which follows the reasoning presented above and includes the often-neglected vertical component of earthquake-generated forces, as urged by Pittelko (1965) and Chopra (1966). The magnitude of k_s is much more difficult to estimate. That its choice is disturbingly arbitrary is clear from the following considerations.

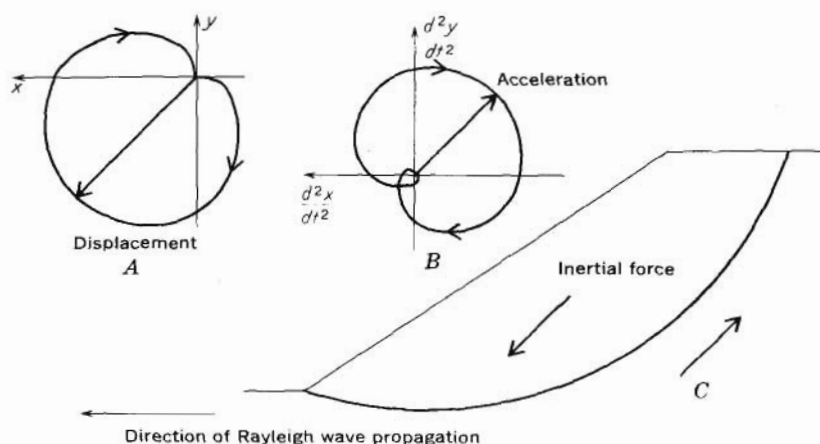


FIGURE 20.—Theoretical particle motion for a Rayleigh wave propagating near the surface, from right to left, far away from the source. *A*, *B*, As the wave passes, a particle undergoes displacements and accelerations, its direction and amount are shown by the vector arrows. Maximum ground acceleration is attained upward and toward the source. *C*, Maximum inertial force in a potential slide is therefore directed down and away from the source. *A* and *B*, from "Reflection and Refraction of Progressive Seismic Waves," by Louis Cagniard. Copyright 1962 by the McGraw-Hill Book Company, Inc. Used by permission of McGraw-Hill Book Company.

During the passage of a seismic wave that propagates normal to the crest of a slope, the body of material within which inertial forces having the same general orientation are generated is determined approximately by the span of one-half wavelength. Within this body the magnitude of inertial force varies both from place to place at any given instant and from instant to instant at any given place. These variations result from the passage of the wavelike impulse and from the variable deformational response of the slope materials according to their geometry and physical properties. Moreover, the configuration of the slope may lead to partial reflection and, thus, during the transit of a series of waves having similar lengths, to the sudden creation of standing waves of augmented amplitude.

Certainly, a choice of k_s such that the constant-added static force equals in magnitude the probable maximum transient inertial force generated by an earthquake would be unduly conservative, as Seed and Martin (1966) pointed out, because a seismic coefficient of 0.1, for example, represents the damaging effects of an earthquake with maximum ground-motion accelerations considerably greater than 0.1 gravity.

Seed and Martin (1966, p. 25) also stated:

During an earthquake, the inertia forces in certain zones of an embankment may be sufficiently large to drop the factor of safety below unity several times but only for brief periods of time. During such periods, permanent displacements will occur but the movement will be arrested when the magnitude of the acceleration decreases or is reversed. The overall effect of a series of large, but brief, inertia forces may well be a cumulative displacement of a section of the embankment; however, once the ground motions generating the inertia forces have ceased, no further deformation will occur unless the soil strength has been decreased significantly.

If the deformations produced are tolerable, then failure—in the sense that limit equilibrium is destroyed and the factor of safety drops for a while below unity—does not necessarily imply impending catastrophe or even major damage. However, reversing stresses, usually produced by earthquake waves, are particularly effective, as Seed and Chan (1966) have shown, in decreasing the effective strength of soils. Furthermore, cyclical-loading tests in the laboratory have indicated that the strength of saturated sensitive clays and of saturated sands, including the Bootlegger Cove Clay and its sand lenses, depends upon the number of stress cycles, as well as on the stress intensity (Seed and Lee, 1966; Seed, 1967; Seed and Wilson, 1967). If a considerable fraction of soil strength is lost by vibration, there arises the possibility of progressive failure and of continued movement even after shaking ceases.

The requisite specialized laboratory testing of locally obtained samples and a thorough dynamic analysis of the west slope of Govern-

ment Hill could not be undertaken on this project. Therefore, a conventional pseudostatic analysis has been used, with some modification, to predict the effects of seismic vibration, and the general conclusions were reviewed with Prof. H. B. Seed in the light of his experience with dynamic testing and analysis of Anchorage materials.

An initial choice of k_s equal to 0.15 vertical and 0.15 horizontal for most analyses herein was deliberately made to gain some idea of how much below 1.0 the factor of safety would fall under extreme conditions. The initial trial is usually followed by an analysis to determine what smaller value of k_s would lead to a factor of safety of 1.0. This typically yielded values of k_s in the range of 0.02 to 0.06. These factors may be compared with empirical design seismic coefficients (horizontal only) of 0.10–0.15 in typical United States practice and 0.15–0.25 in the Japanese earth-dam code requirement, as reported by Seed and Martin (1966); and to the quantity 0.64 times an assumed compressional wave peak acceleration of 0.80g (gravity) used by Seed and Martin (1965) in analysis of the Fourth Avenue slide at Anchorage. The maximum horizontal acceleration at Anchorage during the March 27, 1964, earthquake was estimated, with strong reservations, to be about 0.14g by Cloud (1967), from records made by a strong-motion seismograph at Tacoma, Wash. Long and George (1967a, p. 597) mentioned an analysis of tilted tombstones at Anchorage that indicated a possible maximum acceleration of 0.3g.

The method used in this report for computing active and passive pressures exerted by wedges of frictional or cohesive material is based upon the calculation of pressures exerted on or by a wall if the soil is assumed to adhere to the wall with its full value of cohesion or to have an angle of friction with the wall equal to its own angle of internal friction.

This method seems to be more logical than the use of the usual Rankine expressions for active and passive pressures, although it may be less conservative and may result in higher safety factors.

The general expressions for active pressure E_a and passive pressure E_p are

$$E_a = [\frac{1}{2} \gamma H^2 + p_0 H] [K_{a1}] - cH [K_{a2}]$$

$$E_p = [\frac{1}{2} \gamma H^2 + p_0 H] [K_{p1}] + cH [K_{p2}]$$

where

γ = density

H = height of wall,

p_0 = surcharge per unit area,

c = cohesion, and

K_{a1} , and so on, are coefficients that depend on the assumed angle of internal friction, ϕ .

The values of factors pertinent to the present problems are as follows:

	$\phi=0$	$\phi=35^\circ$
K_{a1} -----	1. 0	0. 25
K_{a2} -----	$2\sqrt{2}$	-----
K_{p1} -----	1. 0	-----
K_{p2} -----	$2\sqrt{2}$	-----

BORING LINE 1

OLD SLIDES

The presence of old slides in the lower part of the slope crossed by boring line 1, indicated by the early topographic map and photographs (pl. 1, figs. 5, 6, 8), is confirmed also by the logs of borings ARR-1A, ARR-1B, and ARR-1C, which were made late in 1966. Summary logs and results of tests on samples from the borings accompany the vertical section (pl. 3). The difference in elevation of the top of the Bootlegger Cove Clay in borings ARR-1A and ARR-1B indicates offset by sliding, and positions of the same contact in boring ARR-1B and in a nearby earlier boring, DM 64-13, suggest a slight backward tilting of the slide block or blocks. No doubt the distribution of the silt and clay beneath the slumped surface of granular materials is more complicated than can be shown on the basis of available information. Regrading has obscured the topographic form of the slides and much material has been removed from the present location of the lumber warehouse. The ground surface as of about 1916 shown on the section is based on an unpublished map prepared by the Alaskan Engineering Commission about 1916, similar to but more detailed than that shown on plate 1. The old slides may have moved along such surfaces as *ABCFDE* or *ABCFG* on plate 3 and *ABOP* in figure 21.

In figure 21 the probable configuration of the pre-1916 slide is shown with an assumed circular arc failure in the Bootlegger Cove Clay. A stability analysis was made to estimate cohesion of the clay, independent of laboratory test results. Also, if it is assumed that the ground surface defined by the 1916(?) contours, and shown by the dotted line, represents the general shape of the slide at cessation of movement ($S.F.=1$), then a measure of the loss of cohesion upon sliding may be estimated, assuming that the angle of internal shearing resistance, ϕ , remains equal to zero. The original face of the bluff is shown as extending from point A' , whose position is determined by the balancing procedure outlined in figure 22, downward to P at a

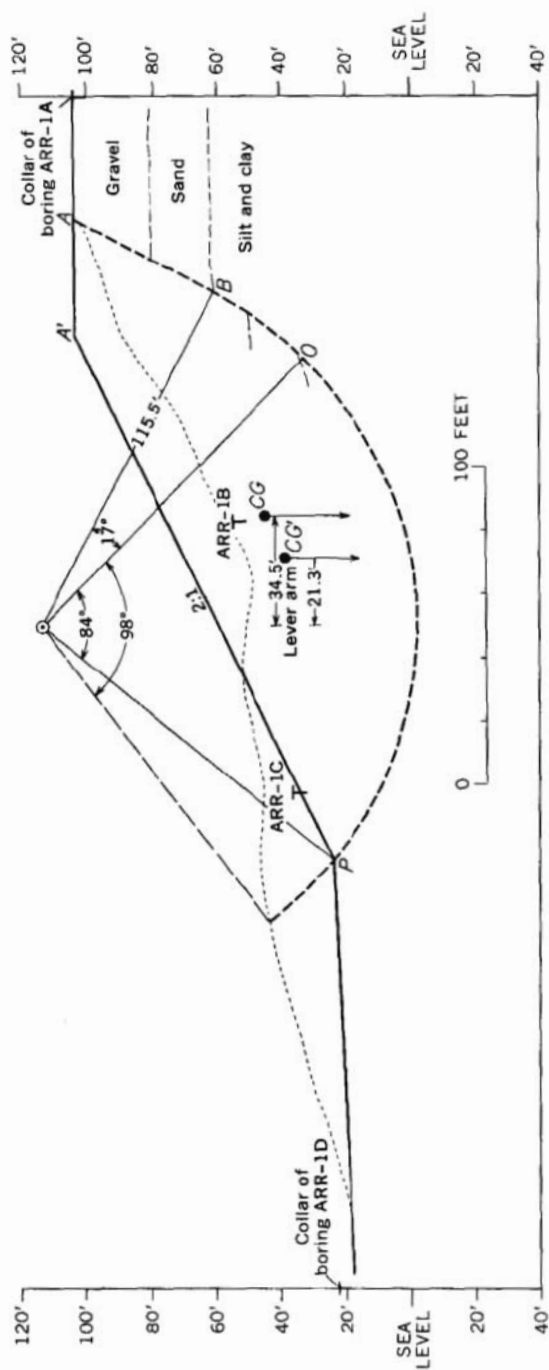


FIGURE 21.—Probable configuration of pre-1916 slide in section along boring line 1. Stability analysis was made to estimate the original cohesion and the amount that cohesive strength decreases upon sliding. Point A', the crest of the slope prior to sliding, was determined by the balancing procedure sketched in figure 22. The assumed original slope is shown by the solid line, and the ground surface after sliding by the dotted line, which is constructed from contours on the Alaskan Engineering Commission's unpublished 1916(?) map.

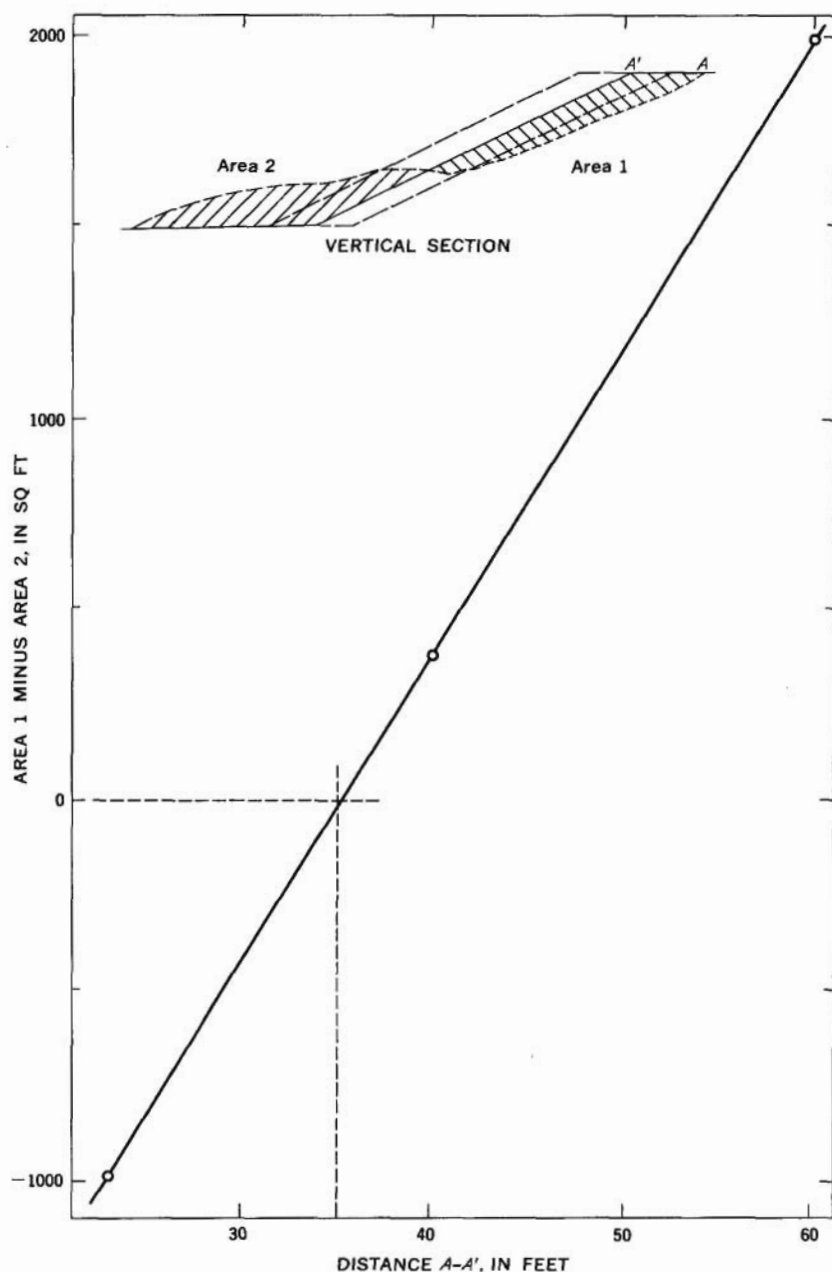


FIGURE 22.—Determination of position of former crest of slope, A' , boring line 1. Various initial positions of the slope are sketched. The one chosen achieves a balance of cross-sectional area between (1) the material that was removed from beneath the original ground surface, at the head of the slide, and (2) the material that came to rest above the original ground surface, in the lower part of the slide. Balance is obtained at 35 feet of retreat of crest.

slope of 2:1. A 2:1 slope is somewhat gentler than the adjacent undisturbed slope to the north and steeper than the slopes on the nose of Government Hill to the south. Unit weight of all materials was assumed to be 125 pounds per cubic foot. Frictional force acting along *AB* in sand and gravel was estimated at 38.4 kips (kilo-pounds). The unit cohesion along arc *BO* was assumed to be 1.5 times that of the clay lower in the section along arc *OP*. Analysis was by static equilibrium of moments, using the center of gravity before and after sliding, as determined by suspending templates of the slide mass, and using before and after weights of 1,251 and 1,107 kips. The position of the sliding surface was estimated. Under the conditions shown and prior to sliding, cohesion of 1,520 psf (pounds per square foot) would have been necessary to maintain a safety factor of 1.0; after sliding, cohesion of 720 psf would suffice to maintain a safety factor of 1.0. This suggests that cohesive shear strength may be decreased by sliding to approximately one-half its original value.

Owing to removal of material from the old slide since 1916, particularly at the toe, and to reconsolidation of soft tidal estuary deposits beneath the coal stockpile that was placed in 1918-21, the most dangerous potential failure surface now probably would crop out east of the warehouse. The stability of several such surfaces is examined in the sections that follow.

CIRCULAR ARC FAILURE, STATIC

The analysis of potential failure along circular arc *ABCJ* (pl. 3), under static conditions, makes use of the basic data shown in table 1.

METHOD 1

Base forces

$$\text{Safety factor} = \frac{(\text{Friction at base of slice 11}) + (\text{cohesion on } BCJ)}{\text{total } W \sin \alpha}$$

$$(1) S.F. = (10.2 + 209) / 157.7 = 1.39 \text{ if wedge } JNHI \text{ is in place.}$$

$$(2) S.F. = (10.2 + 191.5) / 185.9 = 1.08 \text{ if wedge } JNHI \text{ is removed.}$$

Moments about center of arc BCJ

$$\text{Safety factor} = \frac{\text{Total resisting moments}}{\text{Total driving moments}}$$

$$(1) S.F. = [7,030 + (10.2 + 209)100.6] / 21,967 = 1.32 \text{ if wedge } JNHI \text{ is in place.}$$

$$(2) S.F. = [3,127 + (10.2 + 191.5)100.6] / 21,967 = 1.06 \text{ if wedge } JNHI \text{ is removed.}$$

The two ways of calculating by method 1 are mathematically equivalent and agree within the accuracy of estimating locations of centers of gravity of slices.

TABLE 1.—Basic data for analysis of potential failure along arc ABCJ, boring line 1

(α =angle between normal to slip surface and the vertical. Numbers in parentheses are values after removal of prism JNHI if removal of the prism produces changes)

Slice	ϕ	\bar{W} weight (kips)	α°	$\sin \alpha$	$\cos \alpha$	$\bar{W} \sin \alpha$ Tangential component		N component (kips)	Friction $N \tan \phi$	Length contact (ft)	Cohesion (kips)	Lever arm (ft)	Moments (kips-ft)	
						Drive	Resist						Driving	Resisting
11	35	31.6	62.5	0.887	0.462	28.0	14.5	10.2				95.8	3,027	
12	0	82.6	52.5	.793		65.4				34	51	78.3	6,460	
13	0	102.4	36	.588		60.2				25	25	56.3	4,070	
14	0	106.7	23	.391		41.7				22	22	39.3	4,190	
15	0	115	11.3	.196		22.4				21	21	19.3	2,220	
16	0	102	0							20	20	0	0	
(16)	0	(100)	0							(20)	(20)	0	0	
17	0	87.6	-12	.308			18.2			21	21	21		1,840
(17)	0	(87.6)	(-11)	(.191)			(12.6)			(21)	(21)	(19)		(1,280)
18	0	72.6	-23.5	.399			28.8			22	22	40		3,900
(18)	0	(45.1)	(-23)	(.391)			(17.6)			(22)	(22)	(36)		(1,715)
19	0	22.3	-35.8	.584			13.0			27	27	58		1,290
(19)	0	(2.5)	(-32.6)	(.537)			(1.3)			(9.5)	(9.5)	(53)		(132)
						217.7	60.0 (31.8)					209.0 (191.5)	21,967	7,030 (3,127)

METHOD 2

Polygons of forces

- (1) Figure 23

 $S.F. = 1.44$ if wedge *JNHI* is in place.

- (2) Figure 24

 $S.F. = 1.15$ if wedge *JNHI* is removed.

The two methods agree in indicating that failure along arc *ABCJ* under static conditions is unlikely unless the toe of the slope is removed. If the ground was removed to the level of *GH* (base of warehouse), the stability along arc *ABCJ* (through the removal of wedge *JNHI*) would be reduced markedly.

According to the stability computations that follow, failure along circular arc *ABCJ* under seismic conditions seems to be less probable than failure along an almost horizontal surface. Nevertheless, figure 25 shows that the mass above circular arc *ABCJ* has a safety factor of only 0.83 with respect to available cohesion, if combined seismic coefficients of 0.15 horizontal and 0.15 vertical are used in stability computations. If the available cohesion were completely used, an estimated seismic coefficient on the order of 0.06–0.065 would reduce the safety factor to a seismic value of 1.0 from its static value of 1.44.

Possibly, arc *ABCJ* is not the critical arc for the profile on line 1, and some other arc may have a lower factor of safety.

FAILURE ALONG A FLAT SURFACE

Analysis of potential failure along the flat surface *KLM* under static conditions was limited to determining the probable depth of *LM* (pl. 3).

Considerations governing location of a surface of failure

Surface of failure:

1. Will be restricted to zone with lowest value of average cohesion (elev +33 to -8).
2. Should stay out of outwash sand and gravel and hence, should be below inferred position of base of sand in pre-1916 slide—that is, below elevation +28.
3. Should stay below probable position of water table.
4. Emergence of slip surface at toe will depend on where passive resistance is least.

Location of least passive resistance

1. For failures along a relatively high surface (pl. 3), the point of upturning *L* will be vertically beneath *Q*, the base of a graded slope.

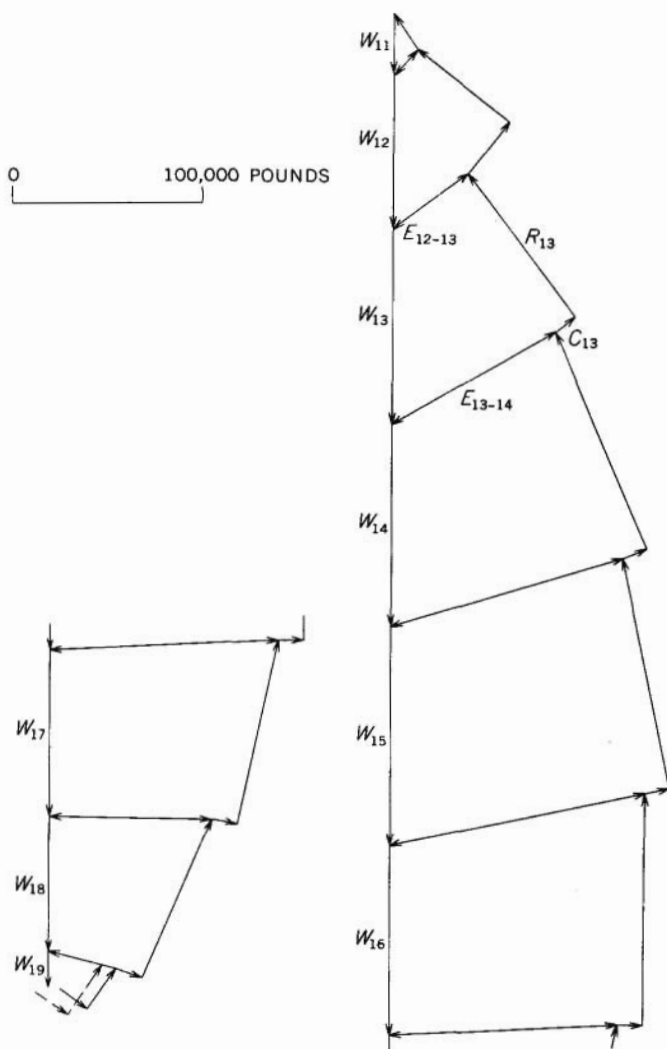


FIGURE 23.—Force-polygon stability analysis of potential failure along circular arc $ABCJ$, line 1, under static conditions, wedge $JNHI$ in place. (See pl. 3.) Assumption that safety factor equals 1.4 (dashed lines, last polygon) leads to excess resistance; assumption that safety factor equals 1.5 (solid lines) leads to deficiency. True safety factor is about 1.44.

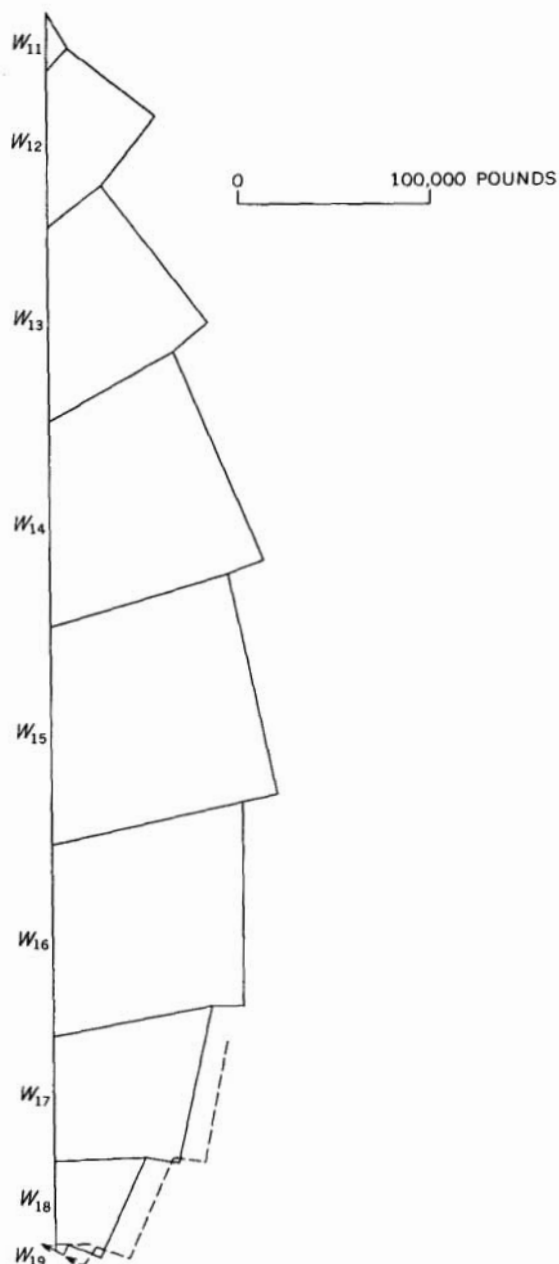


FIGURE 24.—Force-polygon stability analysis of potential failure along circular arc $ABCN$, line 1, under static conditions, wedge $JNHI$ removed. (See pl. 3.) Assumption that safety factor equals 1.1 (solid lines) leads to excess resistance of 5,600 pounds; assumption that safety factor equals 1.2 (dashed lines in last polygons) leads to deficiency of 6,000 pounds. True safety factor is about 1.15.

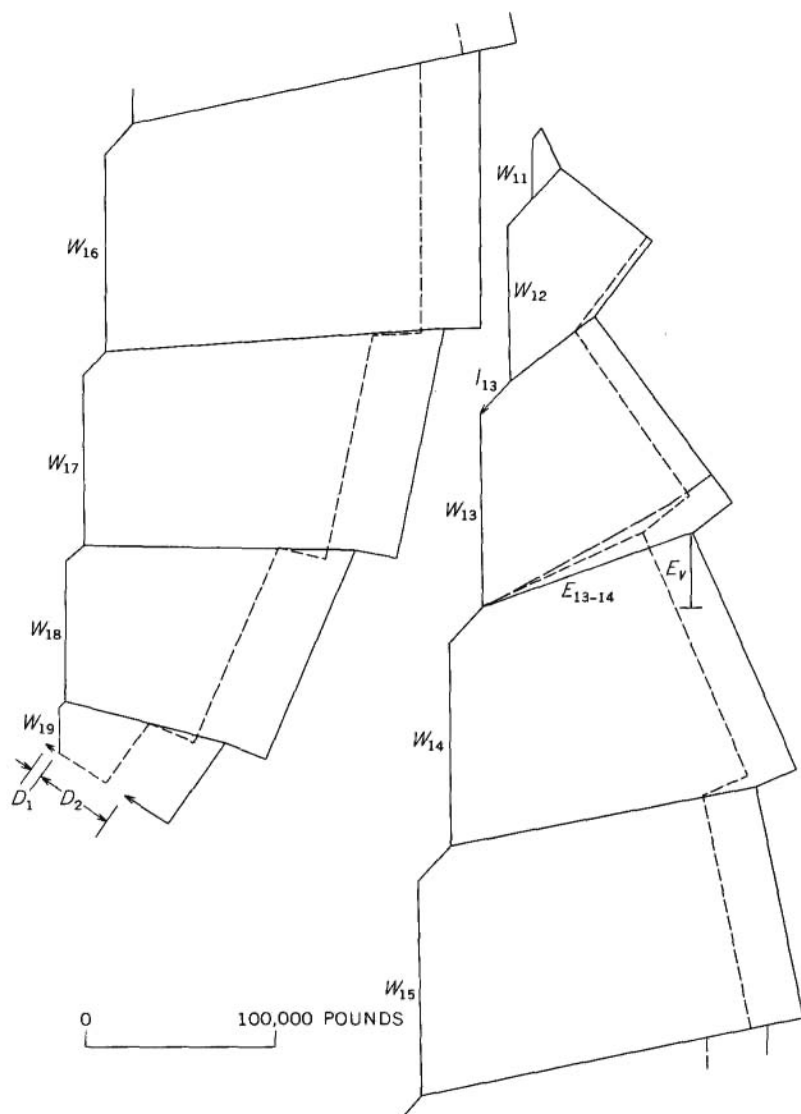


FIGURE 25.—Force-polygon stability analysis of potential failure along circular arc $ABCJ$, line 1, under seismic coefficients of 0.15 horizontal and 0.15 vertical. Inertial forces are shown by force vectors, such as I_{13} . Assumption that safety factor equals 0.8 (short dashes) leads to excess resistance, D_1 , of 7,000 pounds. Assumption that safety factor equals 1.0 (solid lines) leads to deficiency, D_2 , of 41,000 pounds. True safety factor is about 0.83 with respect to available cohesion. Direction of action of E_{13-14} is lowered from long dashed line so that vertical force component, E_v , on face 13-14, does not exceed available cohesion.

2. Unless cohesion drops to a low value, a location for L farther toward the northwest (left) is safer than beneath Q , as more cohesive resistance is mobilized along the longer path.
3. The depth of L below Q will be determined by the relation between passive resistance on QL , cohesion available on surface southeastward (right) from L , and active pressure at head of slide.

Location of most unsafe active head

1. Point of upturning of failure surface (pl. 3) will probably be at point M , vertically below crest of slope.
2. Selection of point M farther to the southeast (right) would lead to no greater active pressure (under static conditions) and would allow more cohesion to be mobilized on slip surface.
3. If M were farther northwest (left), the active pressure would be less because of the decrease in height of slope.

Elevation of zone of probable failure

1. Surface of potential failure will be taken to be at the shallowest location of LM at which active pressure on MA (E_a), requiring mobilization of block $MSRA$, exceeds passive resistance on LQ (E_p) plus cohesion on LM . (See fig. 26; app. A.)
2. Driving component of weight due to seaward dip of bedding of about 1° is neglected.

Depth of LM

The depth of LM shown on plate 3 was chosen so that safety factor is 1.0 for assumed conditions.

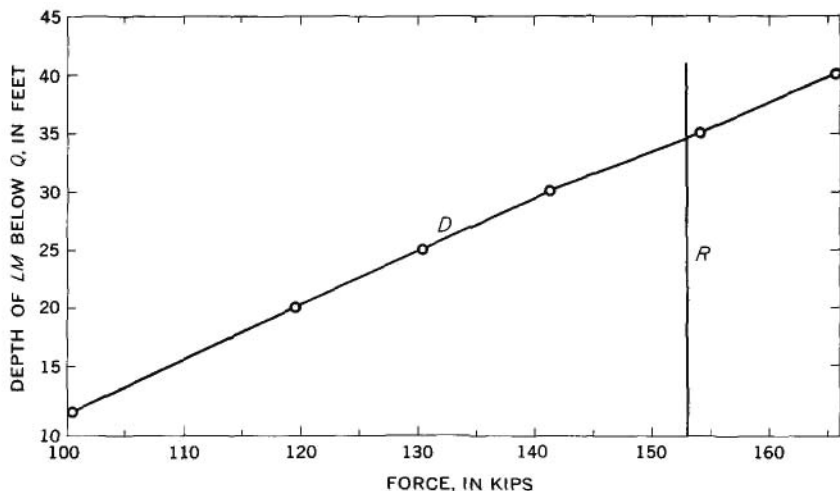


FIGURE 26.—Determination of depth of potential failure surface LM , boring line 1, for static conditions. Depth must be such that driving force ($E_a - E_p$) shown by D line exceeds resistance offered by cohesion along LM shown by R line.

The analysis of potential failure along planar surface $K'L'M'$ under seismic conditions assumes seismic coefficients of 0.15 horizontal and vertical. A surface of failure shallower than the surface of potential static failure was selected because experience has shown that seismic failure will occur as high as possible in the weak part of the Bootlegger Cove Clay. Moreover, liquefaction of thin sand layers is more easily induced, the lower the confining pressure (Seed and Lee, 1966). The segment $L'M'$ along the surface $K'L'M'S'R'$ selected for analysis passes through a wet sandy zone encountered in boring ARR-1B, at depth L' below Q of 17 feet.

Safety factor = Resisting forces/driving forces

Resisting forces = Cohesion of 153 feet times 1,000 pounds cohesion per foot + passive resistance E_p of $QL'K$ 63.2 kips (app. A, item 3).

Driving forces = Active force E_a on $AM'S'R'$ of 190.0 kips (app. A, item 2) + inertial force of material above $K'L'M'S'R'$ of 1,288 kips (app. A, item 4).

$$S.F. = (153 + 63.2) / (190.0 + 1,288)$$

$$S.F. = 0.56$$

The cohesion required to achieve a safety factor of 1.0 is 2,240 psf, which appears to be much more than is available.

The seismic coefficient (horizontal and vertical) that can be tolerated, assuming a unit cohesion of 1,000 psf and a safety factor of 1.0, is 0.047. The computations indicate also that the seismic coefficient that can be tolerated for planar failure is less than that for failure along a circular arc.

Potential failures extending farther southeast and involving masses within about one-half the length of the earthquake waves from the base of the slope would require even higher values of cohesion to achieve stability.

BORING LINE 2

OLD SLIDES

A vertical section along boring line 2 is shown on plate 3 together with summary logs of the borings and test results. The boring logs, observed scarps at points L and P , the Alaskan Engineering Commission's (1916) 1914 and unpublished 1916(?) topographic maps, and information from aerial photographs taken before the surface was altered have been used to arrive at the geological interpretation shown on the section.

As less than one-half of the silt and clay in the section penetrated was logged and sampled, any correlation between borings necessarily must be done almost on a statistical basis. Table 2 lists items believed

TABLE 2.—*Numbered items in logs of borings ARR-2A, ARR-2B, and ARR-2C used to correlate between borings*

Item	Description	Elevation in boring (ft)			Difference in elevation (ft)	
		ARR-2A	ARR-2B	ARR-2C	Between ARR-2A and ARR-2B	Between ARR-2B and ARR-2C
1	Base of outwash sand and gravel.....	75	65	32	10	33
2	Increase in reaction.....	58-59	50-52	18-25	6-9	25-34
3	Highest sand and clay.....	57	49	22	8	27
4	Decrease in consistency.....	47	38-42	13-15	5-9	23-29
4A	Increase in consistency.....		34	9		25
4B	Fluctuation in reaction.....	43-46	32-35	8-9	8-14	23-27
4C	Low water content.....		29	4-8		21-25
5	Base of prominent sand bed.....	37	24	4	13	21
6	Top of thinly bedded sands and clay.....	31	19	-6	13	25
7	Lowest remolded strength.....	26	13	-12	13	25
8	Increase in sensitivity.....	26	13	-12	13	25
9	Increase in shear strength.....	2	-1		3	
10	Increase in sensitivity.....	2	-1		3	
11	Increase in reaction.....	1	-2		3	
12	Decrease in consistency.....	1	-2		3	
13	Lowest thin-bedded sand and clay.....	1	-3 to -5		4-6	
14	Increase in shear strength.....	-13 to -19	-13 to -18		0-1	
15	Highest stones in clay.....	-17	-22		5	

to be of aid in the correlation between borings along line 2; these items are numbered in the summary logs of lithology and test results shown on plate 3 and are described in table 2. Any one of these items, other than the easily recognized base of the sand and gravel, is by itself open to serious doubt. As a group, however, they present a fairly consistent pattern.

Item 1, the base of outwash sand and gravel, suggests a vertical offset between borings ARR-2A and ARR-2B of 10 feet, ARR-2B down; and this interpretation is supported by the eight other features in items 2-8, which indicate an average drop of 10.7 feet. A small and not very fresh appearing scarp is near point *L*, and an old surface of sliding *LN'C'* is postulated (pl. 3).

Item 1 (pl. 3; table 2) also indicates that the ground around boring ARR-2C may have dropped as much as 33 feet relative to that around boring ARR-2B. An offset of about 25 feet is indicated by the average of 10 features in items 2-8. The difference in these offsets may be due to natural irregularity in the erosional surface on the top of the Bootlegger Cove Clay. An observed scarp at *P* on the brushy steep slope

suggests an old surface of sliding that is indicated on the section as extending from *P* to a point below *P'*.

Items 9-15 (pl. 3; table 2) indicate no more vertical difference between the sections in borings ARR-2A and ARR-2B than that attributable to natural variations and to original, seaward dip of the beds. Therefore, if sliding has occurred between borings ARR-2A and ARR-2B, the sole of the slide must be between items 8 and 9—that is, between elevations +26 and +2. The disturbed zone noted from the sample removed from point *C* in boring ARR-2B had a high liquidity index and soft consistency and may be a locus of actual or potential bedding-plane slippage. This planar zone of potential failure has been presumed, for purposes of making stability analyses, to extend southeastward (right, pl. 3) from point *A* beneath the toe of the slope in the pond, past point *C* in boring ARR-2B, and through a disturbed zone at depth 101 feet (elev +12) in boring ARR-2A.

Results of stability analyses for several assumed modes of failure along boring line 2 are given in tables 3 and 4.

CIRCULAR ARC FAILURE

Analysis of potential failure along circular arc *RSP* under static conditions and by use of the method of moments is given in table 3 and shown in figure 27. The safety factor is 1.06. Analysis of potential failure along a somewhat higher circular arc, *AXYZ*, under static conditions and using the method of force polygons yields a safety factor of 1.09. Analysis by the method of moments gives a safety factor of 0.91, and analysis by the method of forces on the base of slices, a safety factor of 0.94. All analyses indicate marginal stability for the assumed conditions. No attempt was made to find the potentially most dangerous circular arc.

Analysis of potential failure along circular arc *RSP* under seismic conditions, assuming seismic coefficients to be 0.15 horizontal and 0.15 vertical and using the method of moments, is given in table 4. The safety factor is 0.7. Seismic coefficients of only 0.018 can be tolerated if a safety factor of 1.0 is assumed and if shear strength is not diminished by seismic activity.

FAILURE ALONG A FLAT SURFACE

Analyses of potential failure along a horizontal or nearly horizontal plane *ABC* prolonged were made for both static and seismic conditions.

The calculations in appendix B and figures 28 and 29 result in the following safety factors for static conditions:

For failure along	Safety factor
ABCDE.....	1.68
ABCJK.....	1.45
ABC'L.....	1.40
ABTW.....	2.75

TABLE 3.—*Stability analysis by moments about center of arc RSP, boring line 2, static conditions—moments of slices*

[See also fig. 27]

Slice	Area (sq ft)	Density (lb per cu ft)	Weight (kilopounds)	Lever arm (ft)	Moments (kilo foot-pounds)	
					Driving	Resisting
1a	1,032	130	134.1	97	24,600	-----
1b	940	127	119.4			
2a	452	130	58.7	62	14,800	-----
2b	1,420	127	180.3			
3	1,018	127	129.3	22	2,840	-----
4a	256	62.5	16.0	22	-----	352
4b	120	120	14.4	29	-----	418
4c	240	127	30.5	13	-----	397
5a	280	62.5	17.5	59	-----	1,033
5b	600	120	72.0	62	-----	4,460
6a	176	62.5	11.0	93	-----	1,023
6b	312	120	37.4	88	-----	3,290
<hr/>						
Arc	Length (ft)	Cohesion (per ft)	Total cohesion (kilopounds)			
PP'	29.6	500	14.8	125.5	-----	33,800
P'R'	241	1,000	241			
R'R	27.4	500	13.7			
<hr/>					42,240	44,773

Safety factor = $44,773/42,240 = 1.06$.TABLE 4.—*Calculation of stability along arc RSP, boring line 2, assuming seismic coefficients of 0.15 horizontal and vertical*

[See also fig. 27]

Slice	Weight (kips)	Vertical force (kips)	Lever arm (ft)	Hori- zontal force (kips)	Lever arm (ft)	Additional mo- ments (kips-ft) due to seismic forces	
						Driving	Resisting
1	253.5	38.0	94	38.0	49.5	5,450	-----
2	239.0	35.8	62	35.8	61.5	4,420	-----
3	129.3	19.4	22	19.4	66	1,706	-----
4a	16	2.4	22	Not counted	-----	-----	50
4b	14.4	2.2	29	2.2	75	165	64
4c	30.5	4.6	13	4.6	75	345	60
5a	17.5	2.6	59	Not counted	-----	-----	153
5b	72	10.8	62	10.8	78.5	848	669
6a	11	1.7	93	Not counted	-----	-----	158
6b	37.4	5.6	88	5.6	79.5	445	487
Shaded area fig. 27	679	Balances		101.8	100	10,180	-----
						23,559	1,641
Static moments						42,250	44,870
						65,809	46,511

Safety factor = $46,511/65,809 = 0.7$. Safety factor becomes 1.0 if seismic coefficients are reduced to 0.018.

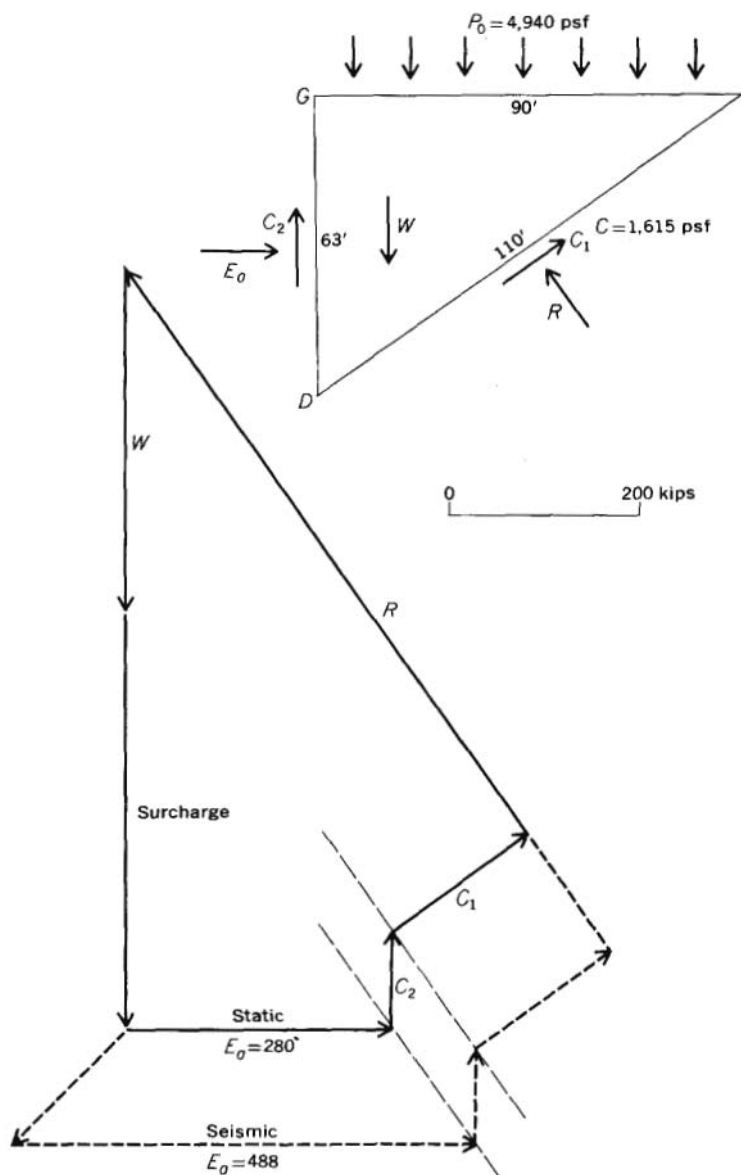


FIGURE 28.—Graphical determination of active pressure E_a on GD , boring line 2.

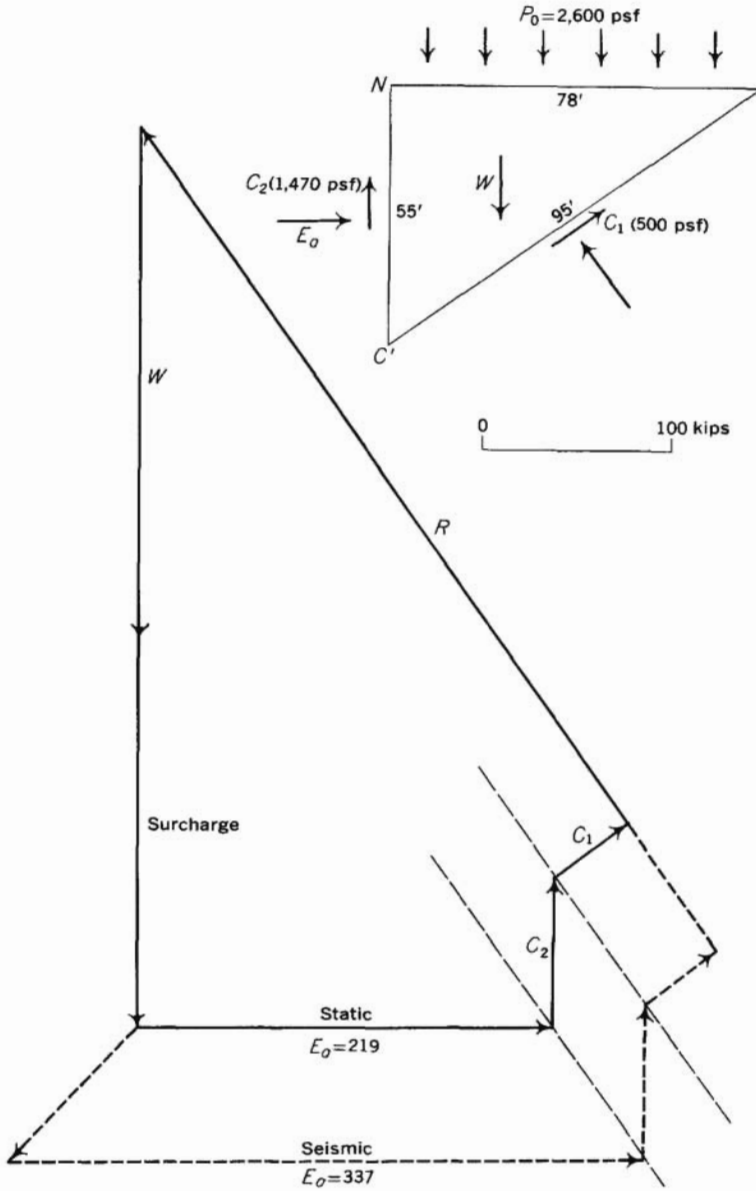


FIGURE 29.—Graphical determination of active pressure E_a on NC' , boring line 2.

4. The hillside was found to be unstable for circular arc failure if seismic coefficients on the order of 0.06 horizontal and 0.06 vertical combined are used in stability computations and was found to be unstable for failure along a flat surface at smaller seismic coefficients.
5. Failure under strong motion probably would not be confined to the slope but would involve, also, part of the level surface back of the crest.

BORING LINE 2

1. Surface expressions of scarps, topographic form, and boring correlations indicate that at least two old slides are on this slope.
2. The lower part of the slope—from Army Road to the pond—verges on instability under static conditions, and slip along a circular arc is the most probable mode of failure near the toe.
3. Possible failure of the rest of the slope up to and beyond boring ARR-2A has been investigated for a nearly horizontal plane at an elevation of about +10, which seems to be one of the more hazardous potential failure surfaces. The slope is stable along this plane under static conditions. The slope is found to be unstable along this plane if seismic coefficients of about 0.035 horizontal and 0.035 vertical, combined, are used in stability computations for assumed failure as far as the south edge of Bluff Road.

GENERAL REMARKS

The areas crossed by boring lines 1 and 2 and the entire stretch of slopes along the west side of Government Hill from Ship Creek around to the military petroleum-product storage tanks have slid in the past. The stability analyses indicate that many of these failures may well have been triggered by earthquakes, although slope failure without quakes is known to be common.

In event of an earthquake a slope will stand or fall according to its physical condition and to the forces imposed on it. The variation in effects of the March 27, 1964, earthquake can be regarded as a result of different physical conditions of the slopes. Equally significant, however, is the possibility that similar slopes were subjected to widely different accelerations, which depended on their position relative to complexly reflected and interfering surface and body waves. Moreover, the seismic forces on an earthbank depend not only on the relatively unchanging influence of topography and geology, but also on factors that vary from one earthquake to another, such as distance, direction of transmission of energy, intensity, period, and type of wave. That a slope did not fail in the severe quake of March 27, 1964, is no guarantee that it is seismically stable. The same slope might fail

under locally higher or more unfavorably directed forces generated by a smaller quake with a different epicenter. Nevertheless, whatever the computations in this report may indicate, the slopes clearly have enough margin of stability to withstand some additional (but unknown) loading equivalent to that resulting from the 1964 earthquake, if conditions affecting stability have not changed since then.

Previous failure does not guarantee stability. The L Street, Fourth Avenue, Government Hill School, and Native Hospital slides each occupied, or partly occupied, sites of previous slides. Many other existing slides were not reactivated. Sliding may interrupt the continuity of soft zones along bedding and help promote future stability. It also may disrupt internal drainage and promote high pore water pressures and future instability. The effects of a previous earthquake, even though they did not result in failure, may reduce resistance to failure in the future.

Loading the toe of a slope may not increase stability as much as expected. Improvement depends very much on the characteristics of the material forming the slope, the degree of saturation, and the shapes of potentially dangerous sliding surfaces. For example, weight added to the lower, upwardly rotating part of a circular arc slide clearly adds to the resisting force and increases stability. If, however, failure is probable along a weak horizontal layer that passes beneath the area being loaded, the addition of more load does no good. It is necessary to intercept the weak layer and to support its overlying material by a buttress that has sufficient shear strength. Should there be, also, a higher weak zone, the possibility of failure along a surface above the buttress must also be considered.

OTHER ENGINEERING GEOLOGIC PROBLEMS

The need for information on the stability of slopes in the vicinity of boring lines 1 and 2 required that attention be focused on the actual and potential landslides of the area. Brief mention is appropriate, however, of other engineering geologic problems that may affect use of the land.

Slides in the shore area.—The possibility of slides along the shore needs to be considered, particularly where slopes below high-water level are naturally steep or have been dredged, and where the shore is loaded with thick fill or heavy structures.

Drainage.—The progressive disruption of the natural drainage in recent years is evident from aerial photographs. (See figs. 10–14.) Part of this derangement is the result of new fills, dikes, and roads. It is possible that much of the standing water could be removed, and that ponds could be at least partly drained prior to filling them in. Improved drainage would decrease hazards of instability and aid in

the rapid attainment of near-final settlement under newly erected fills and structures.

Tectonic warping.—The whole waterfront area is now about 2 feet lower, relative to the sea, than it was prior to the 1964 earthquake. The possible effect of this level change on the soil stability relation of changing ground-water levels to the geologic setting need to be determined by continued observation.

SUGGESTIONS CONCERNING FUTURE DEVELOPMENT

Although the present investigation was directed particularly at the Terminal Reserve lands held by The Alaska Railroad, the following remarks are believed to be applicable to much of the waterfront area—that is, to lands held also by the city of Anchorage and the U.S. Department of Defense. Certainly, any action taken by one group in this area, either beneficial or otherwise, can affect the others, and all face common problems that are often best solved by common action.

For ease of reference the area can be divided roughly into three zones, each of which presents somewhat different problems:

- Zone 1. From 200 yards back of the top of the bluff to 100 yards in front of the bluff toe. Consists of outwash gravel underlain by Bootlegger Cove Clay. The slopes are highly modified by landsliding and artificial fill.
- Zone 2. From 100 yards in front of the bluff toe to MHHW (mean higher high water). Consists of fill, marsh, peat, and estuarine sediments, probably interbedded with material that has slid from the retreating bluff. Underlain by Bootlegger Cove Clay.
- Zone 3. Seaward of MHHW. Consists of fill, estuarine sediments, and slide material, underlain by Bootlegger Cove Clay.

A thorough engineering geologic study of the whole port area should be made. Meanwhile, the present investigation has led to these conclusions:

1. The geologic setting, the topographic cul-de-sac form of the port area, the already large concentration of petroleum handling and storage installations, and the importance of the docks, railroad, and transshipment facilities to the economy of the State dictate that more than ordinary prudence be used in planning and carrying out industrial development.
2. Petroleum storage tanks, other heavy structures, or thick fills should not be placed in zones 1, 2, or 3 unless detailed geologic and engineering studies confirm that the potential problems have been fully evaluated, that the proposed construction is safe, and that it will cause no unfavorable effects to other areas.

3. The toe of the slope in zone 1 should not be cut into, unless measures are taken to fully compensate for the increased landslide hazard caused therefrom.
4. The surface and shallow subsurface waters in zones 2 and 3 and along the bluff face in zone 1, especially at the top of the Bootlegger Cove Clay, should be intercepted and led off without allowing them to reenter the ground. Particular attention should be given to effective disposal of water from the Elmendorf Air Force Base storm drain.
5. A sewerline runs through the slide area crossed by boring line 1, near boring ARR-1B. The Elmendorf Air Force Base sewerline passes under the large fill southeast of City Dock. These and other drains and sewerlines that enter or are in the waterfront area should be checked periodically for possible distress caused by ground creep or consolidation of the surrounding soil.
6. The location and discharge of springs in the tidal zone should be determined so that provision can be made to relieve pressure and remove the water before the springs are covered by impervious fills.

SUGGESTIONS FOR FUTURE STUDIES

Only a part of the investigations planned or proposed in 1966 and 1967 could be accomplished in the available time. An excellent topographic base map was prepared, and the boring, sampling, and testing program along boring lines 1 and 2 was concluded in contracts between The Alaska Railroad and private firms. The results of the exploration and testing programs were analyzed. Conventional geologic mapping was found to be impractical in useful detail on the brush-covered landslide slopes of Government Hill and was of doubtful value on the flats, where large changes in the pattern of fills are occurring rapidly. Nevertheless, a thorough and continuing engineering geologic study of the whole port area, relating and interpreting all existing surface and subsurface information and test results, and obtaining new information as necessary, is essential to future orderly, economic, and safe development.

Periodic vertical large-scale aerial photography would be helpful in many investigations related to land use.

A plan should be made for relating water-level fluctuations in holes in zone 2, and perhaps part of zone 3, among themselves and with tide levels. This plan should give some information on in-place permeability. It would help in laying out and determining the effectiveness of drainage, yield information useful in stability analyses, and make it possible to determine how placing fills on the shore affects the water table at higher elevations on the flats. It would be advantageous to

have piezometers installed in some of the holes. The safety of hydraulic fills against liquefaction during earthquakes should be checked.

A method should be outlined for detecting horizontal and vertical movements in some of the major structures of the waterfront area, including points on the principal docks and on tanks within each of the larger tank farms. A good horizontal and vertical control net should extend eastward beyond the top of the bluffs and should tie to stable points well outside the waterfront and to the city's survey system.

REFERENCES

- Alaskan Engineering Commission, 1916, Reports of the Alaskan Engineering Commission for the period from March 12, 1914, to December 31, 1915 (maps in portfolio): U.S. 64th Cong., 1st sess., House Representatives Doc. 610, pt. 2, Washington, U.S. Govt. Printing Office, 210 p.
- Berg, G. V., and Stratta, J. L., 1964, Anchorage and the Alaska earthquake of March 27, 1964: New York, Am. Iron and Steel Inst., 63 p.
- Brevdy, June, 1964, Alaskan Project, 1964, Target vulnerability studies, recovery research: San Francisco, U.S. Naval Radiological Defense Lab., 106 p.
- Cagniard, Louis, 1962, Reflection and refraction of progressive seismic waves (translated and revised by E. A. Flinn and C. H. Dix): New York, McGraw-Hill Book Co., 282 p.
- Chopra, A. K., 1966, The importance of the vertical component of earthquake motions: Seismol. Soc. America Bull., v. 56, no. 5, p. 1163-1175.
- Cloud, W. K., 1967, Strong-motion and building-period measurements, in Wood, F. J., ed., The Prince William Sound, Alaska, earthquake of 1964 and aftershocks: U.S. Dept. Commerce Environmental Sci. Services Adm. Pub. 10-3 (C&GS), v. 2, pt. A, p. 319-331.
- Clough, R. W., and Chopra, A. K., 1966, Earthquake stress analysis in earth dams: Am. Soc. Civil Engineers Proc., Jour. Eng. Mechanics Div., EM 2, p. 197-212.
- Eckel, E. B., 1967, Effects of the earthquake of March 27, 1964, on air and water transport, communications, and utilities systems in south-central Alaska: U.S. Geol. Survey Prof. Paper 545-B, 27 p.
- Engineering Geology Evaluation Group, 1964, Geologic report—27 March 1964 earthquake in Greater Anchorage area: Anchorage, Alaska, prepared for and published by Alaska State Housing Authority and the City of Anchorage, 34 p.
- Fisher, W. E., and Merkle, D. H., 1965, The great Alaska earthquake: Kirkland Air Force Base, N. Mex., U.S. Air Force Weapons Lab., Research and Technology Div. Tech. Rept. AFWL-TR-65-92, v. 1, 100 p.; v. 2, 312 p.
- Hansen, W. R., 1965, Effects of the earthquake of March 27, 1964, at Anchorage, Alaska: U.S. Geol. Survey Prof. Paper 542-A, 68 p.
- Long, Erwin, and George, Warren, 1967a, Buttress design earthquake—induced slides: Am. Soc. Civil Engineers Proc., Jour. Soil Mechanics and Found. Div., SM 4, p. 199-609.
- 1967b, Turnagain slide stabilization, Anchorage, Alaska: Am. Soc. Civil Engineers Proc., Jour. Soil Mechanics and Found. Div., SM 4, p. 611-627.
- Lowe, John, 3d, 1967, Stability analysis of embankments: Am. Soc. Civil Engineers Proc., Soil Mechanics and Found. Div., SM 4, p. 1-33.

- Miller, R. D., and Dobrovolsky, Ernest, 1959, Surficial geology of Anchorage and vicinity, Alaska: U.S. Geol. Survey Bull. 1093, 128 p.
- National Board of Fire Underwriters and Pacific Fire Rating Bureau, 1964, The Alaska earthquake, March 27, 1964: Distributed by American Insurance Assoc., 465 California St., San Francisco, Calif., 35 p.
- Pittelko, H. P., 1965, Vertical forces in the Alaska earthquake: *Civil Eng.*, v. 35, no. 1, p. 56-58.
- Seed, H. B., 1966, A method for earthquake resistant design of earth dams: *Am. Soc. Civil Engineers Proc., Jour. Soil Mechanics and Found. Div.*, SM 1, p. 13-41.
- 1967, Slope stability during earthquakes: *Am. Soc. Civil Engineers Proc., Jour. Soil Mechanics and Found. Div.*, SM 4, p. 299-323.
- Seed, H. B., and Chan, C. K., 1966, Clay strength under earthquake loading conditions: *Am. Soc. Civil Engineers Proc., Jour. Soil Mechanics and Found. Div.*, SM 2, p. 53-78.
- Seed, H. B., and Lee, K. L., 1966, Liquefaction of saturated sands during cyclic loading: *Am. Soc. Civil Engineers Proc., Jour. Soil Mechanics and Found. Div.*, SM 6, p. 105-134.
- Seed, H. B., and Martin, G. R., 1965, An analysis of the Fourth Avenue and L Street slide areas, Anchorage, Alaska, App. D, in *Remolding of Bootlegger Cove Clay with explosives, preliminary stabilization studies for the Turnagain buttress*: Shannon and Wilson, Inc., for U.S. Army Engineer District, Anchorage, Alaska, 22 p.
- 1966, The seismic coefficient in earth dam design: *Am. Soc. Civil Engineers Proc., Jour. Soil Mechanics and Found. Div.*, SM 3, p. 25-28.
- Seed, H. B., and Wilson, S. D., 1967, The Turnagain Heights landslide, Anchorage, Alaska: *Am. Soc. Civil Engineers Proc., Jour. Soil Mechanics and Found. Div.*, SM 4, p. 325-353.
- Shannon and Wilson, Inc., 1964, Report on Anchorage area soil studies, Alaska, to U.S. Army Engineer District, Anchorage, Alaska: Seattle, Wash., 109 p., app. A-K, 285 p.
- Steinbrugge, K. V., Manning, J. H., and Degenkolb, H. J., 1967, Building damage in Anchorage, in Wood, F. J., ed., *The Prince William Sound, Alaska, earthquake of 1964 and aftershocks*: U.S. Dept. Commerce Environmental Sci. Services Adm. Pub. 10-3 (C&GS), v. 2, pt. A, p. 7-217.
- Stephenson, J. M., 1964, Earthquake damage to Anchorage area utilities—March 1964: Port Hueneme, Calif., U.S. Naval Civil Eng. Lab. Tech. N-607, 17 p.
- Varnes, D. J., 1968, Alaska Railroad Terminal Reserve, Anchorage, Soil stability study; Stability in the vicinity of Boring Lines 1 and 2: U.S. Geol. Survey open-file report, 64 p.

APPENDIXES A-C

APPENDIX A

1. Calculation of forces plotted in figure 26. For example: At depth of L of 12 feet below Q .

- a. Passive resistance at toe.

Cohesion of sand and gravel in upper 2 feet is neglected.

$$\begin{aligned}
 E_p &= \frac{1}{2} \gamma H_1^2 K_{p1} + cH_2K_{p2} & \phi &= 0 \\
 & & K_{p1} &= 1, K_{p2} = 2\sqrt{2} \\
 &= 9,000 + 28,300 & H_1 &= 12 \text{ feet}, H_2 = 10 \text{ feet} \\
 & & c &= 1,000 \text{ psf} \\
 &= 37.3 \text{ kips} & \gamma &= 125 \text{ pcf}
 \end{aligned}$$

- b. Active pressure at head.

Depth is 76 feet, of which 42 feet is in gravel and sand, and 34 feet is in clay.

$$\begin{aligned}
 E_{ag} \text{ (gravel and sand)} &= \frac{1}{2} \gamma H^2 K_{a1} & \phi &= 35^\circ \\
 & & K_{a1} &= 0.25 \\
 E_{ag} &= \frac{1}{2} \times 125 \times 42^2 \times 0.25 \\
 &= 27.6 \text{ kips; horizontal component 22.6 kips}
 \end{aligned}$$

$$\begin{aligned}
 E_a \text{ (clay)} &= \left(\frac{1}{2} \gamma H^2 + p_0 H \right) (K_{a1}) - cH (K_{a2}) \\
 \phi &= 0, & K_{a1} &= 1, & K_{a2} &= 2\sqrt{2} \\
 H &= 34 \text{ feet}
 \end{aligned}$$

$$\begin{aligned}
 p_0 &= \text{surcharge of gravel and sand on clay} \\
 &= 42 \times 125 = 5,250 \text{ psf}
 \end{aligned}$$

$$\text{avg } c = \frac{(1,500 \times 28) + (6 \times 1,000)}{34} = 1,410 \text{ psf}$$

$$\begin{aligned}
 E_{ac} &= \left(\frac{1}{2} \times 125 \times 34^2 + 5,250 \times 34 \right) \times 1 - (2.83 \times 1,410 \times 34) \\
 &= 250.8 - 135.7 = 115.1 \text{ kips}
 \end{aligned}$$

$$\Sigma E_a = 22.6 + 115.1 = 137.7 \text{ kips}$$

- c. Cohesion along LM .

$$\text{Resistance} = 1,000 \times 153 = 153 \text{ kips}$$

$$d. E_a - E_p = 137.7 - 37.3 = 100.4 \text{ kips.}$$

Similarly, $E_a - E_p$ for greater depths of L below Q are also shown below and are plotted in figure 26. Driving forces exceed cohesive resistance on LM at a depth of 34–35 feet.

Depth of L below Q (feet)	Forces, in kips		
	E_a	E_p	$E_a - E_p$
12.....	137.7	37.3	100.4
20.....	195.3	75.9	119.4
25.....	234.5	104.2	130.3
30.....	277.7	135.5	142.2
35.....	324.1	170.0	154.1
40.....	373.2	207.5	165.7

2. Active pressure on $AM'S'R'$, boring line 1, seismic coefficients of 0.15 horizontal and vertical.

- a. Due to gravity and vertical acceleration.

$$E_{ag} = 22.6 \times 1.15 = 26.0$$

$$E_{ac} = (\frac{1}{2} \times 125 \times 1.15 \times 39^2) + (5,250 \times 39) - (2.83 \times 1,360 \times 39)$$

$$= 109,325 + 204,750 - 150,103$$

$$= 164.0 \text{ kips}$$

$$\Sigma E_a = 164.0 + 26.0 = 190.0 \text{ kips}$$

- b. That due to horizontal acceleration is included in inertia of total mass above $K'L'M'S'R'$.

3. Passive resistance of $QL'K'$.

$$E_p = (\frac{1}{2} \times 125 \times 1.15 \times 17^2) + (1,000 \times 15 \times 2\sqrt{2})$$

$$= 20,770 + 42,420$$

$$E_p = 63.2 \text{ kips}$$

4. Weight of material above $K'L'M'S'R'$.

<i>Slice</i>	<i>Weight, in kips</i>
6.....	2.3
7.....	48.8
8.....	119.0
9.....	155.0
10.....	178.8
11.....	176.0
12.....	144.0
13.....	114.0
14.....	90.2
15.....	83.8
16.....	67.1
17.....	57.5
18.....	42.5
19.....	8.8
	<hr/> 1,287.8

APPENDIX B

[Calculation of stability for potential failure on horizontal surface ABC prolonged, boring line 2, static conditions]

1. Failure along $ABCDE$ (pl. 3).

a. $ABCD$ assumed horizontal, which it may not be, quite.

b. Active pressure on DF .

On FG

$$E_a = \frac{1}{2} \gamma H^2 K_{a1} \quad \phi = 35^\circ$$

$$K_{a1} = 0.25$$

$$= \frac{1}{2} \times 130 \times 38^2 \times 0.250$$

$$= 23,400 \text{ lb; horizontal component} = 19.2 \text{ kips}$$

On GD

$$E_a = \frac{1}{2} \left(\gamma + \frac{2p_0}{H} \right) H^2 - 2\sqrt{2} cH$$

$$\phi = 0$$

$$\text{where } \gamma = 127 \text{ pcf}$$

$$H = 63 \text{ feet}$$

$$E_a = 564,000 - 288,000$$

$$p_0 = \text{surcharge}$$

$$= 276,000 \text{ lb}$$

$$= 38 \times 130$$

$$= 4,940 \text{ psf}$$

$$\text{across beds } c = \frac{(26 \times 1,000) + (37 \times 2,000)}{62} = 1,615 \text{ psf}$$

$$\text{Total driving force} = 295,200 \text{ lb}$$

c. Resisting forces.

$$\text{Shear strength on } AH = 0.72 \times 2,000 \times 114.5 = 165,000$$

$$HI = 0.47 \times 2,000 \times 264.5 = 248,600$$

$$ID = 0.36 \times 2,000 \times 113 = 81,400$$

$$\underline{495,000 \text{ lb}}$$

d. Static safety factor.

$$S.F._{ADE} = \frac{495}{295} = 1.68$$

2. Failure along *ABCJK*.

a. Driving forces same as above.

b. Resisting forces.

$$\text{On } AH \text{-----} = 165,000$$

$$\text{On } HI \text{-----} = 248,600$$

$$\text{On } IJ = 0.36 \times 2,000 \times 21 \text{-----} = 15,100$$

c. Static safety factor. 428,700 lb

$$S.F._{AJK} = \frac{428.7}{295.2} = 1.45$$

3. Failure along *ABC'L*.a. Assume failure along old slip plane believed to crop out at *L*.b. Active pressure on *MN* (approx).

$$E_a = \frac{1}{2} \times 130 \times 15^2 \times 0.271 = 3,960 \text{ lb; horizontal component } 3,250 \text{ lb}$$

c. Active pressure on *NC'*.

failure is assumed along an old and presumably softened slip plane. The shear resistance on this surface is estimated at 0.25 tons per sq ft and, after initial failure, to be independent of mean stress ($\phi=0$ on slip surface).

See figure 29.

$$E_a = 219,000 \text{ lb}$$

d. Total driving force, horizontal = $3,300 + 219,000 = 222,300$ lb.

e. Resisting forces.

$$\text{On } AH = 165,000$$

$$HC' = 145,800$$

$$\hline 310,800 \text{ lb}$$

f. Static factor of safety.

$$S.F._{ABC'L} = \frac{310.8}{222.3} = 1.40$$

4. Failure on *ATW*.a. Active pressure on *UV*.

$$E_a = \frac{1}{2} \times 130 \times 14^2 \times 0.25 = 3,180; \text{ horizontal component} = 2,680 \text{ lb}$$

b. Active pressure on *TU*.

$$E_a = \frac{1}{2} \left(\gamma + \frac{2p_0}{H} \right) H^2 - 2\sqrt{2} cH \quad H = 59 \text{ feet}$$

$$= 329,000 - 245,000$$

$$= 84,000$$

$$p_0 = 14 \times 130 = 1,820 \text{ psf}$$

$$c = 1,470 \text{ psf}$$

c. Total driving force = 86,700 lb.

d. Resisting forces.

$$\begin{array}{rcl} \text{Along } AH & \text{-----} & = 165,000 \\ HT = 0.47 \times 2,000 \times 78 & = & 73,400 \\ & & \hline & & 238,400 \text{ total lb re-} \\ & & \text{resisting} \end{array}$$

e. Static safety factor.

$$S.F._{ABTW} = \frac{238.4}{86.7} = 2.75$$

APPENDIX C

[Calculation of stability for potential failure along horizontal surface *ABC* prolonged, boring line 2, seismic conditions]

1. Failure along *ABC'L*.

a. Weight above slip plane (excluding active wedge).

Block	Area (sq ft)
<i>MC'TV</i> -----	5, 580
<i>VTHO</i> -----	4, 860
<i>OHA</i> -----	2, 910

$$\begin{array}{rcl} 13, 350 \text{ sq ft} \times 128 & \text{(approx)} & \\ \text{avg } \gamma & & \\ = 1,710,000 \text{ lb} & & \\ \times 0.15 \text{ seismic coefficient} & & \\ \hline \end{array}$$

256, 500 lb horizontal inertial
force

b. Active force on *MNC'*.

On *MN*

$$E_{ag} = (3,250 \times 1.15) + 0.15 \text{ weight} = 5.1 \text{ kips}$$

On *NC'*

$$E_{ac} = 337,000 \text{ by graphical solution shown in figure 29.}$$

c. Total horizontal driving force.

$$\begin{array}{rcl} 256.5 & & \\ 5.1 & & \\ 337.0 & & \\ \hline 598.6 \text{ kips} \end{array}$$

d. Resisting force.

Assume cohesion not diminished by shaking.

$$\text{On } AH = 165,000$$

$$HC' = 145,800$$

$$\hline 310,800 \text{ lb}$$

e. Seismic safety factor.

$$S.F._{ABC'L} = \frac{310}{598.6} = 0.52$$

f. Seismic coefficient, k , that can be tolerated if cohesion remains unaffected, and $S.F. = 1.0$.

$$1,710k + 3.3(1+k) + 9.1k + 219 + 475.2k(1 + \tan 35^\circ 16') = 310.8$$

$$k = 0.035$$

2. Failure along $ABCDE$.

a. Weight above slip plane (excluding active wedge).

$$W = \text{weight above } AC'M + \text{weight of } C'MFD$$

$$= 1,710,000 + 128 \times 222 \times (171 + 101)/2$$

$$= 5,575,000 \text{ lb}$$

$$\times 0.15 \text{ seismic coefficient}$$

$$\hline 936,250 \text{ lb horizontal inertial force}$$

b. Active force on FGD .

$$\text{On } FG$$

$$E_a = 19.2 \times 1.15 + \text{weight} \times 0.15 = 41.1 \text{ kips}$$

$$\text{On } GD$$

See figure 29.

$$E_a = 488,000 \text{ lb}$$

c. Total horizontal driving force.

$$936.3$$

$$41.1$$

$$\hline 488.0$$

$$1,465.4 \text{ kips}$$

d. Resisting force.

Assume cohesion not diminished by shaking.

$$\text{On } AH = 114.5 \times 0.72 \times 2,000 = 165,000$$

$$HI = 264.5 \times 0.47 \times 2,000 = 248,600$$

$$ID = 113 \times 0.36 \times 2,000 = 81,400$$

$$\hline 495,000 \text{ lb}$$

e. Seismic safety factor.

$$S.F._{ADE} = \frac{495}{1,465} = 0.34$$

f. Seismic coefficient, k , that can be tolerated if cohesion remains unaffected, and $S.F. = 1.0$.

$$5,575k + 19.2(k+1) + 126.8k + 280 + 804.6k(1 + \tan 35^\circ 16') = 495$$

$$k = 0.028$$

